12-13-2002

Short Term Observations of In Vitro Biocorrosion of Two Commonly Used Implant Alloys

Hsin-Yi Lin

SHORT TERM OBSERVATIONS OF *IN VITRO* BIOCORROSION OF TWO COMMONLY USED IMPLANT ALLOYS

by

Hsin-Yi Lin

A Dissertation
Submitted to the Faculty of
Mississippi State University
in Partial Fulfillment of the Requirements
for the Degree of Doctor of Philosophy
in Biomedical Engineering
in the Department of Agricultural and Biological Engineering

Mississippi State, Mississippi

December 2002

SHORT TERM OBSERVATIONS OF *IN VITRO* BIOCORROSION OF TWO COMMONLY USED IMPLANT ALLOYS

by

Hsin-Yi Lin

Approved:

Joel D. Bumgardner, Associate Professor of Biomedical Graduate Program and Biological Engineering Department (Director of Dissertation)	Kirk H Schulz, Head and Professor of Chemical Engineering Department (Committee Member)
A. Jerald Ainsworth, Professor of CVM Basic Science Department (Committee Member)	S.D. Filip To, Associate Professor of Biomedical Graduate Program and Biological Engineering Department (Committee Member)
Robert Cooper, Professor of CVM Clinical Science Department (Committee Member)	David Wipf, Associate Professor of Chemistry Department (Committee Member)
Steven H. Elder, Assistant Professor of Biomedical Graduate Program and Biological Engineering Department (Committee Member)	Jerome Gilbert, Graduate Coordinator of Biomedical Graduate Program of Agricultural and Biological Department

A. Wayne Benett, Dean of College of Engineering

Name: Hsin-Yi Lin

Date of Degree: December 13, 2002

Institution: Mississippi State University

Major: Biomedical Engineering

Major Professor: Dr. Joel Bumgardner

Title of Study: SHORT TERM OBSERVATIONS OF *IN VITRO* BIOCORROSION OF TWO COMMONLY USED IMPLANT ALLOYS

Pages in Study: 109

Candidate for Degree of Doctor of Philosophy

Orthopedic metal implant materials may mediate a variety of adverse tissue reactions by releasing ions through corrosion. Adverse tissue reactions include inflammation, fibrosis and hypersensitivity, which may eventually lead to implant failure.

The goal of this study was to provide a better understanding of the cellular-material interaction at the metal surface. The hypotheses were that the attachment of macrophages on alloy surfaces and their released reactive inflammatory compounds alter alloys' corrosion and surface properties and that changes in corrosion and chemical properties of the surfaces affect cell behaviors. To evaluate these hypotheses, a electrochemical corrosion cell was used to evaluate how cell culture medium, macrophage cells and macrophage cells activated to simulate inflammation affected the corrosion and surface properties of Co-Cr-Mo and Ti-6Al-4V and how released alloy corrosion products affected cell behaviors. The alloy corrosion properties were evaluated by measuring the open circuit potential (OCP), charge transfer, metal ion release, and changes in alloy surface

oxides. Proliferation, viability and metabolism were used to evaluate effects of corrosion products on the cells.

The OCP of Co-Cr-Mo remained unchanged whereas that of Ti-6Al-4V increased over three days for all three test conditions. Both alloys cultured with medium had the lowest OCP among all conditions. With activated macrophage cells, both alloys had the lowest total charge transfer and metal ion released. This improved corrosion resistance was mostly due to an enhancement of the surface oxide due to the reactive species released from activated cells, as indicated from the surface analyses. Both alloys were found to have increased atomic percentage of O and Ti or Cr peaks, which indicated an increase of Ti and Cr oxides.

Corrosion products released from the alloys over three days were very low and did not affect macrophage cell viability, NO and iATP release, which is consistent with the good biocompatibility of these alloys. However the IL-1β released from the activated cells were higher on the alloys compared to the controls.

The data support the hypothesis that cells affect alloy corrosion and surface properties. However cell activities were not affected by these changes over three days.

DEDICATION

For my loving and supporting family in Taiwan; friends from the department: Courtney, Keertik, Marcia, Kori, Paul, Brad, Daniel and Shawn and all my friends in the Taiwan Student Association in Mississippi State University, especially Dr. and Mrs. Su. Most important, to my academic advisor Dr Joel Bumgardner for his tremendous amount of support and encouragement.

ACKNOWLEDGMENTS

The author expresses her sincere gratitude to the many people without whose assistance this dissertation could not have completed. First of all, sincere thanks to my academic advisor and committee chair, Dr. Joel D Bumgardner, for his spending time and effort to guide me and support me through the doctoral program; providing opportunities for attending conferences and extracurricular learning experiences. Thanks to Dr. Kirk Shultz, Esteban and Holly for making available the XPS instruments used in the study and spending time for data analysis. Appreciation is also due to the members of my dissertation committee, Dr. Jerald Ainsworth, Dr. Robert Cooper, Dr. Steven Elder, Dr. David Wipf, and Dr. Jerome Gilbert. Finally, thank the grant support from the Whitaker Foundation.

TABLE OF CONTENTS

LIST OF TABLES

TABLE Page

LIST OF FIGURES

FIGURE Page

FIGURE Page

CHAPTER I
BACKGROUND

Biocompatibility has been defined as the state of mutual coexistence between the biomaterials and the physiological environment such that neither has an undesirable effect on the other (Tang *et al.* 1995; Santerre *et al* 2000; Amstutz *et al.* 1992; Kavanagh *et al.* 1994). For orthopedic implant materials, biocompatibility depends on both mechanical and corrosion/degradation properties. Implant devices for large joints such as knees and hips are composed of metals/alloys to support heavy loads and stresses. Cobalt- and titanium-based alloys are widely used in orthopedic devices due in part to their high strength and fatigue properties. Improper placement or fixation of the devices or gross elastic dissimilarity between the material and bone are of concern and may contribute to osteoporosis and bone atrophy through stress shielding of the bone (Williams, 1987). Besides their high strength and fatigue properties, the cobalt and titanium based alloys also have excellent corrosion resistance. Cobalt-based alloys depend on a protective chromium oxide for their corrosion resistance and titanium-based alloys depend on a protective titanium surface oxide. Corrosion of orthopedic implant materials results in the release of metallic ions, such as Co, Cr, Ni, Al and V, which have the potential to cause hypersensitivity, toxicity and carcinogenic reactions (Hallab *et al.* 2001; Kanerva *et al.* 2001; Granchi *et al.* 2000; Schedle *et al.*1998; Signorelo *et al.* 2001; Memoli *et al.* 1986). For these reasons, careful *in vitro* and *in vivo* testing is important to assess the health

and risk benefits of these materials and their degradation products.

Corrosion of Biomaterials and Product Distribution

The nature of body chemistry is considered complex and highly variable due to the variety of different salts (NaCl, KCl, $CaCl_2$ etc.), proteins (albumin, fibrin, collagen etc.), cells (osteoblasts, fibroblasts, monocytes etc.) and cell activities (tissue remodeling, immune responses, wound healing, neural activities etc.). It has long been recognized that this situation can be highly significant for implant alloy corrosion processes. For example, H^+ and Cl^- ions, which are abundant in normal physiological environment, are known to accelerate the dissolution of metal ions from implant alloys; in a solution with H^+ and Cl^- ions and low in oxygen, the metal ions are more likely to be released from the metal surface into solution (Fontana and Greene 1978) when compared to solutions without these ions. Factors such as low pH, high Cl^- and H_2O_2 concentrations during inflammation and some proteins such as bovine serum albumin may accelerate the *in vivo* corrosion process (Wataha *et al.* 1998; Wataha *et al.* 2001, Clark and Williams, 1982). Active cellular processes may affect corrosion by other routes as well. For example, the local pH decreases during inflammation and this pH shift may disrupt the alloy surface oxides, also known as passive films. The disruption of passive film leads to increased corrosion, causing more metal ion release and more inflammation, leading to a more acidic environment and thus more corrosion (Park 1984).

Metal particles and metal ions are released from implants through uniform dissolution and accelerated corrosion processes such as crevice, pitting, galvanic and fretting corrosion. Dissolution begins early, as soon as the implant comes in contact with

the body fluid/tissue. It involves the general slow release of metal ions from alloy surface. Accelerated corrosion processes are of specific concern since they result in increased material loss which will decrease alloy mechanical properties as well as increase exposure of host tissue to corrosion products.

Pitting is initiated by surface defects and high energy grain boundaries and accelerated by the stagnant flow with presence of corrosive ions and limited oxygen transfer in the pits. Pitting was frequently observed in older stainless steel fracture fixation hardware, e.g., on the underside of screw heads. It may also occur on the neck or the underside of the flange of proximal femoral endoprostheses (Black, 1988). Crevice corrosion occurs between two close surfaces or in constricted places where oxygen exchange is not available. For examples, 16-35% of modular total hip implants demonstrated moderate to severe crevice corrosion in the conical head - neck taper connections (Gilbert *et al*, 1993). Studies of retrieved stainless steel multipart internal fixation devices show visible crevice corrosion at the junction between screw head and the plate in 50-75% of all devices (Black, 1988).

Galvanic corrosion happens between dissimilar metals (alloys) where the more electronegative one becomes the anode and the other becomes the cathode. An example of galvanic corrosion would be a titanium alloy screw in contact with a stainless steel plate (Griffin *et al*, 1983). Fretting occurs between two articulating contact surfaces, for example, the articulating joints of hips and knees, so the surface atoms are constantly being removed and alloy dissolution is accelerated on both surfaces. Fretting corrosion at

the head-neck coupling of a femoral stem and head is an important source of metal release that may lead to increased concentrations of ion in the serum (Brown *et al.* 1981).

The metals of particular concern in joint replacement are Ni, Co, Fe, Cr, Mo, Ti, V and Al since they are the major components of the most commonly used materials in orthopedic implants. Studies have shown elevated metal ions were found within patients with implants. Jacobs *et al.* in 1998 studied the metal-degradation products of total joint replacements. They measured the concentrations of Ti, Al, Co and Cr in the serum and the concentration of Cr in the urine of 75 patients during a three-year study. The results showed that, after 3 years, patients who have a well functioning prosthesis with components containing Ti have as much as a threefold increase in the concentration of Ti in the serum. Those who have a well functioning prosthesis with cobalt-alloy components have as much as a five-fold and an eight-fold increase in the concentrations of Cr in the serum and urine, respectively. They reported that the predominant source of the disseminated Cr-degradation products was probably due to the fretting corrosion at the head-neck coupling instead of passive dissolution of the extensively porous-coated cobalt-alloy stems. In a follow up study, they found patients with failed patellar components made of Ti alloy had a 50 fold higher Ti in serum compared to controls without implants (Jacobs *et al.* 1999). Leopold *et al* (2000) reported a patient with failed metal-backed patellar component had >500 ppb serum Ti concentration. That was 98 times higher than before implant failure and > 100 times higher than patients with well-functioning implant of this type.

Dobbs *et al.* (1980) reported a female patient with two bilateral Co-Cr-Mo total hip replacements, one had been in service for 14 years (metal-on-metal) and the other for 5.5 years (metal-on-plastic). Although the metal-on-metal side had become painful, the patient remained active until she died. The measurements indicated that the concentrations of Co and Cr in the lung, kidney, liver and spleen were up to fifty times "Standard Man" values. High values occurred also in the urine and in the hair. The tissue adjacent to the metal-on-metal joint was heavily laden with metal wear debris, whereas that adjacent to the metal-on-plastic joint was relatively uncontaminated. The concentration decreased with distance from the implant. Co predominated in the urine, whereas Cr predominated near the implants (1 to 100 ppm range).

Bouchard *et al.* (1992) demonstrated that Al^{3+} is selectively leached from Ti-6Al-4V. Concentrations of Al in body fluids observed over multiyear time periods increased with exposure times and fell after implant removal. Elevated Al also was reported in non-articulating Ti-6Al-4V implants *in vitro* (Bruneel *et al.* 1988). Corrosion product containing Al^{3+} from implants is of particular concern because of its toxic effects. The toxicity usually results from its competition with other metal ions (e.g. Mg^{2+}) in enzymes and proteins. The nervous system is especially susceptible to Al^{3+} toxicity. In humans, Alzheimer's disease, dialysis encephalopathy and Parkinson-dementia complex are some examples of maladies linked to Al^{3+} interference.

Ni is a major cause of metal hypersensitivity since 12-15% of normal population is estimated to be allergic to this metal (Merrit 1984; Merrit 1986; Yamamoto 2002). Traisnel *et al.* (1990) reported systemic elevation of Ni and Cr concentration in twelve

patients implanted for eight years with Ni-Fe-Cr intramedullary nails and in twelve patients with Ni-Fe-Cr bone plates for 13 years respectively. They found mostly crevice corrosion with these devices and the metal ion concentrations increased with time. Wataha *et al.* (2001) implanted Ni wire subcutaneously in the rats for 7 days and found released Ni ion (48 μg/g) in tissue caused necrosis and severe inflammation of tissues up to 5 mm away from the wire. The Ni concentration in tissue adjacent to Ni-Cr wire was about 12 times less than that of pure Ni, around 4 μg/g and no signs of damaged tissue. No detectable Ni was found in tissue near polyethylene (control).

Corrosion of implant alloys has been seen in all types of devices in different forms. The corrosion products, including metal ions and particulates, usually accumulate locally and cause inflammation, tissue damage and fibrosis surrounding implants and eventually result in implant failure. It is important to examine the causes and the mechanisms of corrosion *in vivo* and its effects in order to improve the performance of implant devices.

Electrochemical Corrosion Testing

Performing *in vivo* corrosion tests, when compared to *in vitro* tests, are not always possible; it requires more techniques and qualified personnel and is more time consuming compared to *in vitro* tests. On the other hand, *in vitro* corrosion tests can not precisely replicate all the *in vivo* conditions of the implants but they are faster than *in vivo* tests and can target on specific effects of a single factor (pH, Temperature, cells etc.) and usually provides good correlation with *in vivo* cases.

There are several ways to measure and predict the corrosion behavior of medical implant alloys that simulate the *in vivo* situation. For example, Electrochemical Impedance Spectroscopy can be used to approach the oxide's resistance and capacitance as well as model the oxide with a electronic circuit to further predict the corrosion behavior in different conditions. Potentiodynamic test scans through a high amplitude DC voltage and the current vs. voltage curves provide information about the corrosion potential, breakdown potential, repassivation potential, and corrosion current density of the test alloys. The area of hysteresis in current vs. voltage curves indicates the susceptibility of metal to pitting corrosion. Linear polarization tests apply potential 10 mV more and less than corrosion potential to predict the corrosion current from the slope of potential vs. current (slope= 0.026 / corrosion current) (Fontana, 1986); Direct measurement of metal ion concentration in solution using atomic emission spectroscopy or atomic absorption spectroscopy can also be used to correlate to the corrosion current by using the Faraday's Law ($r = iA/nF$; r: corrosion rate ($g/s\text{-}cm^2$); i: current density (A/cm^2); A: atomic weight (g/mole); n: valency (-); F: Faraday's constant (96500 coulomb/mole)). In general, the lower the open circuit potential (E_{corr}) and the higher the corrosion current (i_{corr}) are, the more corrosive the alloys are and thus less desirable for implant applications.

Most *in vitro* corrosion tests are done in simple salt solutions (phosphate buffered solution (PBS), Hank's balanced salt solution (HBSS), artificial saliva etc.) to simulate the ion concentration and pH of body fluids. Ti-6Al-4V tested by potentiodynamic polarization in de-aerated neutral pH Hanks balanced salt solution (HBSS) exhibited

good corrosion properties (Venugopalan and Gayden 2001; Zardiackas *et al*, 1996; Imman and Fraker, 1996). The open circuit potential (E_{corr}) was noble (95 mV vs. standard calomel electrode (SCE)) with low corrosion current density (i_{corr} = 26 nA/cm^2) (Venugopalan and Gayden 2001; Zardiackas *et al*, 1996) and the material translated into a passive behavior without active-passive transition. The alloy did not exhibit a breakdown potential or pitting potential in the range of 0 – 2100 mV vs. SCE, indicating that its surface oxide was very stable and provided the alloy corrosion resistance (Kovacs, 1993). This alloy was also demonstrated to have minimal release of metal ions into the periprosthetic tissue even in an extremely acidic medium (Kolman and Scully 1994). While Ti-6Al-4V exhibits excellent corrosion properties, it is susceptible to fretting corrosion when subject to articulation and is not used for bearing components in articulating implants (Kawalec *et al.* 1995).

Wrought Co-Cr-Mo has a lower E_{corr} (-171 mV vs. SCE) and higher i_{corr} (94 nA/cm^2) values compared to those of Ti alloys (Venugopalan and Gayden 2001; Chohateb *et al*. 1996). This alloy does not exhibit active-passive transition as they are in a passive state prior to testing. The passive region for this material is not as potential independent as Ti-6Al-4V and exhibits a secondary peak at about 500 – 700 mV vs. SCE corresponding to the oxidation reactions of Cr at a higher valence level. There is a transition from passive to transpassive behavior with a breakdown or pitting potential (E_{bd} = 450mV vs. SCE) (Venugopalan and Gayden 2001). It does not exhibit a hysterisis, which means it can repair damage to its passive layer. Co-Cr-Mo alloys have higher wear

resistance than most of the implant alloys and thus are used for making articulating components (Park and Lakes 1992).

Galvanic coupling of implants made of different alloys results in accelerated corrosion. When coupling Co-Cr-Mo with Ti-6Al-4V, the OCP of Co alloy was reported to increase over time (Irby and Marek, 2000), indicating thickening of the surface oxide, whereas OCP of Ti alloy showed an initial maximum and a drop (initial thinning), followed by a slow increase over time (thickening over time). Although the corrosion current was low (~1 $\mu A/cm^2$) for the first hour, with Co alloy being the anode, galvanic corrosion is a major concern for a long term *in vivo* application. Thus coupling different alloys should be avoided for most implant applications.

Corrosion resistance is also affected by other factors such as the chemical composition (Huang, 2002) and the microstructure (Planko *et al.* 1998; Callister 2000) of the alloys. Huang evaluated six Ni based alloys and found only those with Cr concentration as high as 20% were resistant to pitting corrosion and had twice as high passive range compared to other Ni based alloy with Cr only around 13%. Though one of the low Cr specimen contained Ti, which is known to provide excellent pitting corrosion resistance, was not immune to pitting because Ti only composed ~4% of the bulk solution. Microstructures such as grain boundaries, impurities, manufacturing defects and porous structures etc. are all known to increase corrosion (Callister, 2000). Implant materials usually are treated with high temperature during manufacturing and that may alter or cause alloys to rearrange their microstructures and thus change their corrosion resistance (Georgette 1987). Jacobs *et al.* (1990) stated that carbide incorporation may

predispose the Co-Cr-Mo alloys to accelerated intergranular corrosion. Placko *et al.* (1998) reported Co alloys with more Cr carbides in the grain boundaries and finer grains show higher degree of metal ion release over time and more localized attack (pitting) compared to those with less Cr-carbides in the grain boundaries and with larger grain size.

Proteins have been added to test solutions to further simulate the *in vivo* conditions. Proteins are reported to enhance or reduce corrosion of different types of metals (William and Clark 1982) and proteins of different molecular weights also have different efficiencies of combining metal ions (Hallab *et al.,* 2001; Hallab *et al.,* 2001). Mora *et al.* (2002) found that the presence of albumin accelerated copper corrosion at various pH and oxygen concentrations. Wataha *et al*. (2001) demonstrated the importance of defining exactly the composition of biological solutions used to assess *in vitro* corrosion and biocompatibility of dental casting alloys. They found more metal ion release occurred in saline-BSA solutions compared to saline alone for most alloys. The metal ion release was less in the cell-culture medium than in the saline-BSA solution for most elements.

Zhu *et al.* (1999) investigated three types of protein bovine serum albumin (BSA), gamma-globulin and hemoglobin with electrochemical polarization resistance measurements and found the corrosion rate of copper always increased with the presence of proteins and decreased with time; different kinds of proteins showed different dependence on copper corrosion rate. The copper corrosion rate in the presence of gamma-globulin or hemoglobin increased monotonically with increasing concentration of

the proteins and these three proteins shifted the corrosion potential of copper towards negative. Omanovic and Roscoe (2000) used the electrochemical impedance spectroscopy technique to investigate the interfacial behavior of beta-lactoglobulin at an austenitic stainless steel surface over the temperature range 299 to 343 ^{o}C at an open circuit potential. The corrosion resistance value was found to be very sensitive to the amount of adsorbed protein (surface concentration), thus indicating that the adsorption of the protein was accompanied by the transfer of the charge, via chemisorption, and influenced the mechanism and kinetics of the corrosion reaction.

Proteins are abundant in the human body and they deposit onto implant surfaces seconds after implantation prior to cell attachment. With their significant effects on corrosion, attention need to be drawn to proteins as to understand the corrosion behavior of metal implants *in vivo*.

The role of cells on corrosion has not yet been established by corrosion tests. The presence of cells and their metabolism were reported to alter the composition and thickness of surface oxides, thus the alloy corrosion behavior might be different with cells present. There are different cells/tissues surrounding the implant *in vivo* and the effects of different cells/tissues on corrosion should be identified for improved understanding of the performance of implant *in vivo*.

Effects of Metal Ion Release from Implants

The first row of transition metals such as Co, Cr, Cu, Mn and Zn are present in trace amounts in the human body. Zn^{2+} is found in many enzymes and is also present in

insulin. Co^{3+} is found in vitamin B_{12} and Fe^{2+} is present in the hemoglobin molecule of red blood cells. Mg^{2+} is an element of bones and teeth. Mn is essential for healthy bones and Cr^{3+} plays a key role in glucose metabolism. Cu deficiency gives rise to bone disease. Problems with metallic implants arise when corrosion or wear releases metal ions in abnormal locations or in quantities beyond what can be handled by the host. Released metal corrosion products may lead to hypersensitivity, toxicity and/or carcinogenic reactions. Most of these adverse reactions occur near implant sites since most corrosion products accumulate locally. Implants causing hypersensitivity and toxicity reactions eventually need to be removed for causing patient discomfort. For stress bearing orthopedic implants, osseointegration is important for keeping implant in contact with the bone tissue and ensuring proper load transfer. When metal ions accumulate, they activate macrophage cells, which release cytokines (interleukins, PGE_2 etc.) that lead to bone resorption and attracts fibroblasts. Bone atrophy and fibrous tissue (made of fibroblasts, macrophage cells, and damaged cell debris) surrounding implant prevents osseointegration and retards load transfer. Inhibited load transfer further causes bone atrophy and eventually implant failure.

Human and animal studies

Recent studies have suggested that metal ions might bind to proteins as soon as they are released from the metal substrate (Wooley *et al.* 1997; Ingham *et al.* 2000). Metal ions bound to proteins, such as MHC molecules expressed on the surface of immunostimulatory dendritic cells, are known to induce T-lymphocyte responses leading

to type IV hypersensitivity reactions (delayed type hypersensitivity) as illustrated by contact hypersensitivity to metal ions in contact with the skin.

Cr causes cell necrosis, activates phagocytes and leads to inflammation. Savarino *et al.* (1999) and Granchi *et al.* (1999) both suggested the presence of metal ions, especially Cr^{3+}, released from orthopedic implants (Co-Cr-Mo) was associated with a decrease of lymphocyte subpopulation in patients with loose implants. Granchi *et al.* speculated that Co-Cr-Mo implants release metal ions which could mediate the priming or the renewal of a cell-mediated hypersensitivity reaction. Cr^{6+} is very biologically active and is a well-known carcinogenic and mutagenic agent (Kawanishi *et al.* 2002; Liu and Shi 2001; Chen 2001; das Neves 2001; Laffargue 2001). Studies have shown that Cr^{6+} in red blood cells induced cell-specific types of DNA damage (cross-links) in liver in 14-day chick embryos (Misra *et al.* 1994). *In vivo* and *in vitro* Cr^{6+} toxic effects are related to its intracellular reactions. Once inside the cell, it is reduced to stable Cr^{3+} by ascorbate (Diane 1994) or by creating radicals such as OH^{-} (Wink 1994) that can futher damage cells or RNA and DNA. Black suggested that Cr released in the biologically active Cr^{6+} form from their observation of dose-related lung disease and late elevation of the urine/serum chromium ratio seen in animal models (Black *et al.* 1987; Black 1994). As Cr^{5+} and/or Cr^{4+} intermediates have been reported in Cr^{6+} reactions with biological reductants, chromium damage is thought to originate from these chemical species (das Neves *et al.* 2001). Cr^{6+} binds to or enters cells and is not eliminated from the body until the cells are eliminated (Merrit and Brown 1983; Merrit *et al.* 1989). Laffargue (2001) reported a case of malignant fibrous histiocytoma of the bone that developed 20 years

after a femoral fracture treated by stainless steel plate-screw fixation. Dispersion energy spectrometry of intracellular particles on the periphery and at the center of the tumor demonstrated the presence of Cr, Fe and Ni at different concentrations. The presence of metallic components in tumoral cells suggests a possible relationship between metallic implants and malignancy.

The location of the release of aluminum ion may have a marked impact on homeostasis. Aluminum binds to bone and is associated with osteomalacia (which means soft bones, the osteoid does not mineralize properly, usually is related to abnormalities in vitamin D). Aluminum deposits have also been found in brains of healthy individuals. Brain and bone accumulation of Al in patients who are undergoing chronic renal dialysis has been a major concern (Escalas *et al.* 1976; Oppenheim *et al.* 1989). Nasu and Suzuki (1998) studied the mechanism of the inhibition of K^+-induced muscle contraction caused by Al^{3+} in guinea pigs. They also found that with increasing duration of Al^{3+} treatment, Al^{3+} ions accumulate in intracellular compartments and may exert an inhibitory action inside the muscle cells. The possibility of Al from implant material corrosion should be well monitored and the concentration of aluminum should be kept low.

Rostlund *et al*. (1990) evaluated tissues surrounding nitrogen implanted Ti implants inserted in the abdominal wall of rats after 1 and 6 weeks. After 1 week the implants were surrounded by a fluid space containing proteins and scattered macrophages but few polymorphonuclear granulocytes. After 6 weeks the fluid space had largely disappeared around implants. Around the implants, macrophages predominated in the inner zone (within 25 μm from implant surfaces) and multinuclear giant cells were

present in almost all sections. Around the implants, fibroblasts increased and macrophages decreased with increasing distance from the surface. Macrophages close to titanium were large and had an active appearance as indicated by the presence of large amounts of endoplasmic reticulum and large Golgi areas in the cytoplasm.

Al-Bayati *et al.* (1989) observed that Vanadate (V^{5+}) at a dosage concentration of 0.9 mg/kg body weight / day produced acute toxic signs in rats when injected subcutaneously for 16 days. These signs were weakness, loss of appetite, dehydration, significant reduction in body weight, nose bleeding, and death. The pathological and biochemical changes were most severe in kidney tissue. At two days, degenerative and necrotic changes of the renal tubular and glomerular epithelium, thickening of glomerular membrane, vascular congestion, and edema were observed. The renal lesions were coupled with changes in the concentrations of protein, RNA, DNA, and hydroxyproline. Stained tissue sections from liver, lung, heart, spleen, thymus, lymph nodes, testes, and adrenal glands of the treated appeared normal. Biochemically, significant changes in protein, RNA, DNA, and hydroxyproline were also observed in these organs. At lower dosage (0.6 mg V/kg per day for 16 days), similar but less severe pathological and biochemical changes in kidneys and other organs were observed. At 0.3 mg V/kg per day for 16 days, the changes in the tissues were detected only at the biochemical concentration.

Clinical retrieval studies and animal models have shown metal ions released from implants may cause adverse tissue reactions from genetic alteration, cell necrosis to abnormal organ function. Investigations are needed to understand how different cells

react to different ions and their toxicity effects to improve selections of metal materials in applications of implant devices.

In vitro studies

Toxicity effects on cell proliferation and viability

Granchi *et al.* (1998) suggested that if a high amount of Co were released from metallic particles, necrosis and strong inflammation would ensue. If only low concentrations of ions were released, apoptosis would favor a tissue adaptation to the implant because the event is silent and does not lead to danger signals that induce inflammation. In some ways, this result agrees with the *in vivo* data. Inflammatory events periprosthetically have been reported to be rare in the early stages but may occur with increased duration of implantation, whereas the accumulation of metal debris in the draining lymph nodes has been shown to lead to necrosis inflammation.

Bearden and Cooke (1980) exposed fibroblasts to CoCl and NiCl solutions in a concentration range of 7.5 to 30 μg/ml. At all Co concentrations, they observed depressed growth rates. Ni solutions enhanced the cellular growth rates at the lower concentrations of 7.5 μg/ml, but depressed the growth rate at 30 μg/ml.

Metal ions may also contribute to bone resorption by impairing osteoblast growth and function (Lee *et al.* 1997; Wang *et al.* 1996; Liu *et al.* 1999). These reports have demonstrated that Ti and Cr ions increased the release of proinflammatory cytokines such as interleukins and PGE_2 from macrophages that lead to increased bone resorption.

Thompson *et al.* (1996) found that calcium concentrations were reduced when ions from Ti-6Al-4V were added before a critical point of osteoblast differentiation. The results indicated that ions associated with Ti-6Al-4V alloy inhibited the normal differentiation of bone marrow stromal cells to mature osteoblasts *in vitro*, suggesting ion release from implants *in vivo* may contribute to implant failure by impairing normal bone deposition.

The amount of Mo utilized in implant materials is very small and unlikely to cause problems (Evans *et al.* 1986). However more studies are needed on the distribution, elimination and toxicity of Mo.

Toxicity effects on cell ultrastructure and morphology

In vitro investigations examining at the ultrastructural organization of cells as an indication of cell damage have also been conducted. Trump *et al.* (1973) suggested that *in vivo* cell damages due to metal ion exposure, beginning with a normal resting cell and ending in cellular death, were irreversible even if metal ions were removed from the solution later on. Subsequent *in vitro* studies (Frank and Griffin 1985; Messer *et al.* 1999 a/b) showed that cellular ultrastructural damage induced *in vitro* by Co or Ni was similar to the events described by Trump for cells under *in vivo* trauma conditions. Messer *et al.* (1999a) examined the *in vitro* ultrastructural features to components from Ni-Cr dental alloys. It was found that the severity of the cellular response increased when the concentration of the components increased. The dose-response correlation was stronger *in vitro* than *in vivo*. As the severity increased, the cells showed a decrease in rough endoplasmic reticulum, a more diffuse plasma membrane, and a decrease in cellular

organization. Messer *et al.* (1999b) previously reported on the individual effect of each ion and its critical dose. They monitored the changes in metabolic activity of gingival fibroblasts exposed to metal ion solutions and found Cr^{6+} and Be^{2+} were the most toxic, causing cellular alteration at 0.04-12 ppm, followed by Cr^{3+} and Mo^{6+} and Ni^{2+} at 10, 100, and 3-30 ppm respectively. They reported that cytotoxic substances attack at the molecular level, and these effects are reflected in the structure of the cells and organelles. The experiment evaluated the cellular morphology and ultrastructural changes of human gingival fibroblasts exposed to salt solutions of ions important to implant alloys (Cr^{3+}, Cr^{6+}, Ni^{2+} and Mo^{6+}). The effects observed under SEM and TEM included irregular shaped nuclei for cells exposed to Cr^{6+} and Ni^{2+}, pseudopodia for cells exposed to Mo^{2+}, and lipid droplet formation for cells exposed to Ni^{2+}.

Toxicity effects on cell functions

Immune cells

A recent study showed that metal ion release from hip prostheses correlated with a depression of immune system; Donati *et al.* (1998) found Cr, Co and Ni ions in the blood of 17 patients with joint prostheses. They had a significant decrease in leukocyte, lymphocyte and T lymphocyte sub-populations. Cytokine release by lymphocytes (IL-2, IL-4 and IFN-γ), proliferation of T and B cells, and immunoglobulin production by B cells were shown to be significantly inhibited by Ni, Co and Cr ions *in vitro*. Similar

results were seen when debris of titanium and cobalt-chromium alloy were present in the peritoneal cavity of female mice after 12 weeks (Wang *et al.* 1997).

Metal ions were shown to affect the behavior of macrophages and in turn affect the immune responses of the host tissues. Wataha *et al.* reported that metal ions (Ni, Au, Cu) released from dental alloys could activate macrophages to express IL-1β, TNF-α and the result could be amplified with the presence of LPS (Wataha *et al.* 1996 and 1999). They also found that metal ions induced macrophage cytotoxicity such as decrease their enzyme activities (LDH and SDH) and reduced their protein production (Wataha *et al.* 1995).

Osteoblasts

Nichols *et al.* (1997) suggested that instead of activating osteoclasts to cause bone resorption, metal ions such as Ti^{4+}, Al^{3+}, V^{5+}, Cr^{6+} and Mo^{6+} decrease osteoblast activity. Hypersensitivity effects of Co appear to be similar to Ni (Merrit 1987). Co is not generally considered carcinogenic because of the rapid removal. However, *in vitro* studies have indicated that Co produces is more cytotoxic to human osteoblasts than other elements (Mo, Cr, Al, Ti) (Hallab 2002). Morais *et al.* (1998) tested sub-toxic concentrations of Co^{2+} and Cr^{3+} ions on the differentiation of osteoblast cell lines *in vitro*. The 50% toxic dose was 208μg/L for Co^{2+} and 1960 μg/L for Cr^{3+}. At concentrations below these, Co^{2+} inhibited osteoblast differentiation whereas Cr^{3+} has little effect.

These findings suggest metal ions play a role in periprosthetic pathology and contribute to implant failure by impairing bone repair while allowing fibrous tissue formation following debris-induced osteolysis.

Fibroblasts

Doran *et al.* (1998) demonstrated a dose dependent toxicity and neoplastic transformation of $CoCl_2$ and $CrCl_3$ on mouse fibroblast cells; though they only induced transformation at a high concentration; 1200μg/ml. This study did not allow definitive conclusions about the carcinogenic potential of the metal ions but did indicate that Co ion may constitute a hazardous risk for Co-Cr-Mo implants.

In general, tissues exposed to elevated ion concentrations through abnormal pathways such as implant dissolution processes are reported to have adverse tissue reactions. It is still not known how the ions are released and what causes these reactions. This study will provide new information as to possible causes.

Surface Oxides of Implant Alloys and Their Characteristics

For the Co-Cr-Mo and Ti-6Al-4V alloys, corrosion resistance is derived from their ability to form surface oxide films and to retain them under *in vivo* conditions. The surface oxide of the alloys provides a protective layer to prevent the alloys from further corrosion. *In vivo*, it is the surface oxide that directly interacts with the biological environment including proteins, cells and tissues. It can also initiate inflammatory responses as a result of metal ion release from corrosion. Metal ion release from implant

materials can be increased by many orders of magnitude when fresh surfaces are exposed or surface oxides are disrupted as compared to materials with intact, protective surface oxides (Leopold *et al*., 2000; Jacobs *et al*., 1999).

Oxides of implant alloys vary in many ways, including their thickness, elemental compositions and their relative percentages and oxidation states. These variations depend in part on the environment the surfaces contact. For example, tissue metabolic activity was reported to affect the thickness of the surface oxides. Sundgren *et al.*, (1985) reported the thickness of stainless steel surface oxide implanted in bone marrow increase 3-4 times compared to before implantation (5 nm) while it was unaffected when implanted in cortical bones. The reactive chemical compounds such as hydrogen peroxide, superoxide, and nitric oxide from activated macrophage cells further enhanced the metal oxides on the Ti-6Al-4V alloy surfaces (Pan *et al.* 1996 and 1998). Different surface treatments, including different passivation procedures (by using H_2O_2 or HNO_3) (Kilpadi *et al.* 1998; Pan *et al.* 1998) and sterilization processes (heat or UV) (Kilpadi *et al.* 1998, Ohnsorge and Holm 1978, Vezeau *et al,* 1996) have also been reported to change the surface oxides. Pan *et al.* observed Ti oxide increase 10 fold after treated with 100mM H_2O_2 in PBS for 30 days. Kilpadi reported passivation of pure Ti with HNO_3 resulted in thinner and less phosphorous incorporated surface oxide compared to non-passivated Ti and dry-heat treatment increased the oxide thickness compared to non-sterilized specimens.

Milosev *el al*. (2000) found that the oxide layer of Ti-6Al-4V was predominantly TiO_2 and its thickness varied from 2 to 7 nm. They also found that the thickness of the

oxide layer depended on the oxidation potential; the higher the anodic potential, the thicker the surface oxides were. Callen *et al.* (1995) discovered that the nitric acid treatment used to develop surface oxide and corrosion resistance in Co-Cr alloys and stainless steel may not work for Ti alloys. Nitric acid decreased the thickness of Ti-6Al-4V surface oxide layer and increased the release of the trace elements, whereas it had no effect on pure Ti. Another study by Kilpadi *et al.* 1998, though showed that HNO_3 treatment altered the Ti oxide characteristics either directly by altering the oxide structure or indirectly by removing carbonaceous moieties (C=O, C-O, C-C, C-H etc.) that alter the oxide. The surface structure of Ti-6Al-4V has been reported as a porous outer layer and a protective, dense inner layer. Molosev (2000) reported that Al_2O_3 was incorporated in the outer layer close to the solution/oxide interface while TiO and Ti_2O_3 were located in the inner layer close to the oxide/metal interface. Pan (1997) also reported the oxide as a double layer and stated (Pan *et al*., 1998) that the inner layer is responsible for the high corrosion resistance of the alloys.

The surface oxide on Co-Cr-Mo alloys is composed primarily of Cr_2O_3, with $CoCr_2O_4$ and CoO species (Strandman and Landt, 1982). Corrosion resistant oxides were proportional to the chromium content of the alloy, with the most corrosion resistant oxides developing on alloys with between 10-25% Cr. Smith *et al*. 1991, reported Mo to be present only at the oxide-metal interface. Heat treatments from 800-1200^oC increased oxide thickness on Co-Cr-Mo by causing the oxide to grow into the alloy, though no chemical or structural difference between the layers was reported (Strandman and Landt, 1982). Nitric acid passivation not only increases oxide thickness but also increases the O

and Cr content and introduced nitrogen species into the surface oxide. Furthermore, it has been observed that different passivation and or cleaning procedures may remove contaminants, but may introduce others (Smith *et al*., 1991). Strandman and Landt (1982) reported heat treatment of Co-Cr-Mo resulted in the development of two separate layers within the oxide as observed by light microscopy. Smith (1991) reported the surface oxide on Co-Cr-Mo, which was about 5 nm, was relatively thinner than that on Ti alloys. Mo was not seen on the surface before ion sputtering.

Surface oxides may change with their environment and these changes may affect the corrosion performance of the implant devices (Pan *et al*., 1998; O'Brian *et al.* 2002; Sawase *et al.* 2001; Shabalovskava 2002; Mustafa *et al.* 2002). Pan reported increased corrosion potential of Ti alloy after treating the surface with H_2O_2 for 30 days. Sawase used a plasma source ion implantation (PSII) method to increase the thickness of the surface oxide layer. The potentiodynamic polarization measurements in PBS showed improved corrosion resistance *in vitro* and bone formation around this surface-modified specimen in a rabbit model showed that all implants were in contact with bone and had some proportion of bone within the threads after 4 weeks.

The release of metal ions from implant devices into the human body environment is inevitable. Physiological reactions to the metallic species released from medical implants have become a matter of increasing concern; especially inflammatory responses for they are likely to result in implant failure (Gerhardsson *et al.* 2002; Mak *et al.* 2001; Cornelini *et al.,* 2001; Hallab *et al.,* 2001 Esposito *et al.,* 2000). It is still not clear how implant alloys trigger the immune system and how the system responses cause the

implant failure. But since all the interactions occur between the biological environment and the implant surface oxides and/or their byproducts such as metal ions, it is important to understand the mechanisms behind these interactions by characterizing changes in alloy corrosion and surface properties due to host cells/tissues. These data will thus contribute to the improved understanding and performance of implant materials.

Specific Aims

Macrophage cells release NO, inflammatory chemicals (interleukins, PGE_2, TNF etc.) and lower the local pH during stimulation. Among these reactions, the release of NO, an oxidizing agent, may react with surface atoms and change the metal surface oxide thickness and/or composition. Metal corrosion behavior depends on its surface oxide properties and behaviors of macrophage cells may alter the alloys' corrosion behavior by changing its surface oxide and thus affecting metal ion release. Increased ion release may lead to local cell toxicity, chronic inflammation and potentially host tissue hypersensitivity. The released ions and host tissue injury may attract more macrophages to the implant site and could establish a negative feedback loop. This could be the key factor causing chronic inflammation, bone resorption and eventually implant failure.

To investigate these hypotheses (1. cells alter the alloys' surface and corrosion properties and 2. alloys' corrosion products further activate cell immune responses), both corrosion behavior of implant alloys and cell responses to released corrosion products were evaluated. The following specific aims were proposed:

1. To measure the corrosion potentials and total charge transferred of the alloys in three test conditions, namely alloys incubated with medium, macrophage cells and activated macrophage cells.
2. To measure changes in surface oxide of the alloys after incubation with three test conditions.
3. To measure the total amount of metal ion released from each condition over time.
4. To characterize the response of non-activated cells and activated cells after they attach and grow on the surfaces of the glass (control) and test alloys by assessing their viability, intracellular ATP concentrations and released NO and IL-1β concentrations in the supernatant.

This project will provide information on how alloy corrosion behavior effected by the host cells/tissues as well as host responses to implant devices in terms of different surfaces and release of metal ions.

CHAPTER II
MATERIALS AND METHODS

Materials

Alloys

Cobalt-chromium-molybdenum (Co-Cr-Mo) and titanium-6 aluminum-4 vanadium (Ti-6Al-4V) alloys were chosen for use in this study for their outstanding mechanical properties and biocompatibility. The alloys were donated by Allvac Inc., Monroe, NC. Co-Cr-Mo alloy contains 27-30% Cr, 5-7% Mo and Co for balance and has a tensile strength near 655 MPa according to American Society for Testing and Materials (ASTM) F75: Standard Specification for Cast Cobalt-Chromium-Molybdenum Alloy for Surgical Implant Applications. The Ti-6Al-4V alloy contains 5.5-6.5% Al, 3.5-4.5% V and Ti for balance with tensile strength about 860 MPa according to ASTM F136: Standard Specification for Wrought Titanium 6Al-4V ELI Alloy for Surgical Implant Applications.

The alloys were provided in 6" bar stock and cut by a diamond wheel into rectangular plates (4 cm x 4 cm x 0.2 cm) (Figure 1) to fit into a customized electrochemical corrosion cell. The surface area of the alloy in the electrochemical corrosion cell was 14.4 (3.8 x 3.8) cm^2. The plates were prepared by wet polishing through a series of silicon carbide (SiC) sandpaper up to 1200 grit, ultrasonically cleaned for 5 minutes in acetone, ethanol and distilled water to eliminate all the

contaminants on the metal surface. Samples were passivated in 20% nitric acid for 30 minutes at room temperature to mimic the clinical surface treatments according to ASTM F86 – "Standard Practice for Surface Preparation and Marking of Metallic Surgical Implants".

Figure 1. A polished Co-Cr-Mo alloy plate used for corrosion tests. It was wet polished using SiC sandpaper up to 1200 grit, cleaned and passivated according to ASTM F86 to simulate clinical implant surface preparation.

Setup of The Electrochemical Corrosion Cell

A custom made electrochemical corrosion cell (Figure 2) was used to evaluate the role of cells on alloy corrosion. The corrosion cell was designed to simulate the *in vivo* situation of cells growing on an implant material surface. The body of the cell was made of Teflon® with dimensions: 6.36cm x 6.38cm x 4.27 cm. The lid had a port for placement of a salt bridge tube for the reference electrode. It was made of clear Plexiglas® for the convenience of observing cell culture in case of contamination and the positioning of the electrodes. The lid fit loosely enough to allow gas exchange between cultures and the ambient atmosphere in cell culture incubator. Both counter

electrodes were made of graphite and a saturated calomel electrode (SCE) served as the reference electrode. The metal plate was positioned at the bottom of the box, with the treated surface facing up allowing cells to attach and grow on it. A screw was used to provide electrical connection to measure the potential and current of the alloy as well as to immobilize the plate.

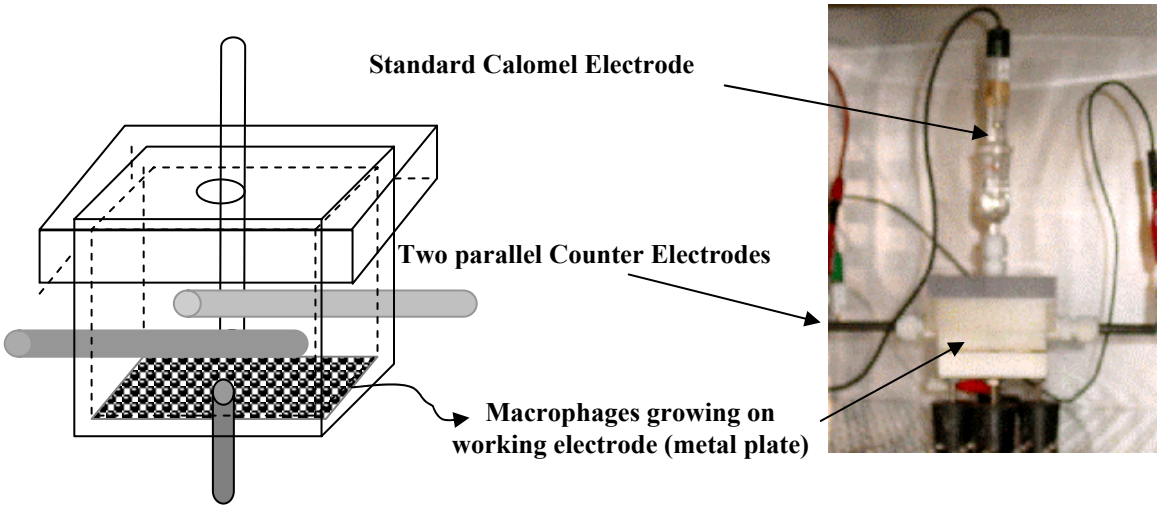

Figure 2. Schematic and image of the electrochemical corrosion cell. The reference saturated calomel electrode (SCE) was inserted from the lid using glass bridge tube fitted with Vycor® tip (96% silica glass, PerkinElmer, TN); two graphite counter electrodes were inserted from the side of the cell and the alloy plate (working electrode) at the bottom of the cell with treated surface facing upward in order to have contact with the cells and medium.

The corrosion cell, including the graphite and working test electrodes and salt bridge were disinfected with 70% of ethanol solution and UV light before assembly in a sterile cell culture hood. The corrosion cell operated in a cell culture incubator (37 ^{o}C, 5

% CO_2, 100 % humidity) during experiments by running wires connecting the electrodes to a potentiostat.

Cells

Macrophage cells are one of the major components in wound healing and inflammatory reactions and are often seen around implant sites. A transformed macrophage cell line (TIB-71, American Type Culture Collection (ATCC), Manassas, VA) was chosen for use in this study because it produces reactive nitrogen species: nitric oxide (NO) and pro-inflammatory cytokine: interlukin-1 beta (IL-1β) at measurable concentrations when activated by exposure to endotoxin and interferon. Reactive oxygen species such as hydrogen peroxide (H_2O_2) and super oxide (O_2.) are also know to be released by this cell line when activated though they are released at lower concentrations as compared to NO (Pfeiffer *et al.,* 2001). Cells were maintained in cell culture medium (Dulbecco's Modified Eagle Medium (DMEM) + 1mM Na-pyruvate+ 10 % fetal bovine serum (FBS) + 1 % Antibiotic-Antimycomic + 2mM L-glutamine) in an incubator at 37^{o}C, 100 % moisture and 5 % CO_2. Cells were activated to release NO and IL-1β to simulate *in vivo* inflammation by using cell culture medium supplemented with 0.05 μg/ml interferon gamma (IFN-γ, R&D System, Minneapolis, MN) + 5 μg/ml lippopolysaccaride (LPS, E. Coli Serotype 0127:B8, Sigma, St louis, MO) (Parker and Bumgardner, 2002). Controls were set up by growing non-activated cells or activated cells on glass petri dishes with the same surface area as the alloys in

the corrosion cell. The surface area to the volume of culture medium was the same as the corrosion cell as well.

Methods

Corrosion Tests- Open Circuit Potential (OCP) (mV vs. SCE) and Direct Current Measurements

OCP is the thermodynamic measurement of how likely the surfaces are to corrode. The more negative OCP is, the more reactive the surface is, but it is not an indication of how fast the corrosion occurs. Corrosion currents are measured to determine the rate of corrosion. Corrosion current is directly proportional to the rate of mass loss according to the Faraday's Law (Boyd and DeVault, 1959): $r = iA/nF$; r: corrosion rate (g /s-cm^2); i: current density (A/cm^2); A: atomic weight (g/mole); n: valency (-); F: Faraday's constant (96500 coulomb/mole).

There has not been any *in vitro* corrosion experiments with macrophages present being conducted previously. Several animal studies have shown that Co-Cr-Mo could cause significant metal ion release in urine and blood serum in three days (Black *et al.* 1987, Brown *et al.* 1993). Besides metal ion elevation can be significant in three days compared to the controls, typical cell seeding density for corrosion tests, around 1 – 5 cells/cm^2, would reach confluency in three days. Over confluent cells will cause cell death and detaching from the surface and affect the corrosion and surface tests. In order to avoid cell death and cell detachment, constant medium changing and cell splitting

were required. To split the cells during the test may have effects on the corrosion test for it may disturb the surface and the position of the electrodes and thus the consistency between tests. For the above reasons, the corrosion test was chosen for three days.

OCP and direct current measurements were conducted over a 72-hr period using a potentiostat (Electrochemical Impedance Analyzer Model 6310, EG&G Instruments, Oakridge, TN). The OCP (mV vs. SCE) was measured for 4 hours and then the current ($\mu A/cm^2$) was measured for 20 hrs at 0.0 V vs. SCE. The OCP and current measurements were repeated on consecutive days for a total of 72 hrs (3 days). The M352 SoftCorr III software (EG&G Instruments Inc., Oakridge, TN) was used to control the experiment and record the potential (mV vs. SCE) and current (μA or nA) over time. The total charge transferred was then calculated by estimating the area under the current vs. time curve and then summed over 3 days. By comparing the OCP and total charge transfer from the test alloys with and without cells (non-activated and activated) attached, the effects on corrosion due to non-activated cells and activated cells was estimated.

For each type of alloy, tests were conducted in cell culture medium, with macrophage cells, and with LPS+IFN-γ activated macrophage cells. The non-activated cells and activated cells were seeded at $1x10^5$ cells/cm^2 in 13 ml medium. With activated cells, the medium was supplemented with 0.05μg/ml IFN-γ + 5ug/ml LPS. For each alloy, each test condition was repeated at least three times.

At the end of each day (24-hr period), the leads to the electrodes were disconnected, the corrosion cell was moved into a sterile hood and a 4 ml aliquot of

medium was collected for nitric oxide, IL-1β and metal ion release analysis. The medium was replaced with fresh medium or medium containing LPS+IFN-γ. Cells were evaluated for viability, morphology and intracellular ATP at the end of each 3-day test.

Analysis of Metal Ion Release

Inductively-coupled plasma atomic emission spectroscopy (ICP-AES) is a multi-element analysis technique that dissociates a sample into its constituent atoms and ions by the high energy of the plasma generated from the argon gas. The atoms and ions are caused to emit light at a characteristic wavelength by exciting them to a higher energy level. This is accomplished by the use of an inductively coupled plasma source, usually argon. The plasma will reach a temperature in the range of 6,000 - 10,000 ^{o}C, which will efficiently atomize most elements. Figure 3 is the schematic of the plasma source. The sample is introduced into the plasma flame as an aerosol by use of a nebulizer to cause characteristic light emissions from the constituent atoms and ions.

A monochromator is used to separate specific wavelengths of interest, and a detector is used to measure the intensity of the emitted light. This information is used to calculate the concentration of the elements in the sample. The resulting detection limits are very low, and they usually range from 1-10 ppb for simple aqueous solutions. Detection limits were ~50 ppb for the culture medium solutions used in this study.

Supernatants collected from tests with and without cells at day 1, day 2 and day 3 during the 3-day corrosion tests were analyzed for metal ion content. A 1:10 dilution of

the supernatants were made using 5% $HNO_{3(aq)}$ before analysis to minimize the interference from the protein and salt in the solution during the analysis. Standards were made in cell culture medium - 5% HNO_3 matched solutions for each ion, Co, Cr, Mo, Ti, Al, and V, to generate emission vs. concentration curves. Each sample was spiked with 100 ppb of each ion for more precise readings since the concentration of these ions were often low (~10-30 ppb range). Spike was subtracted to obtain the amount of ion in solution after the samples were read.

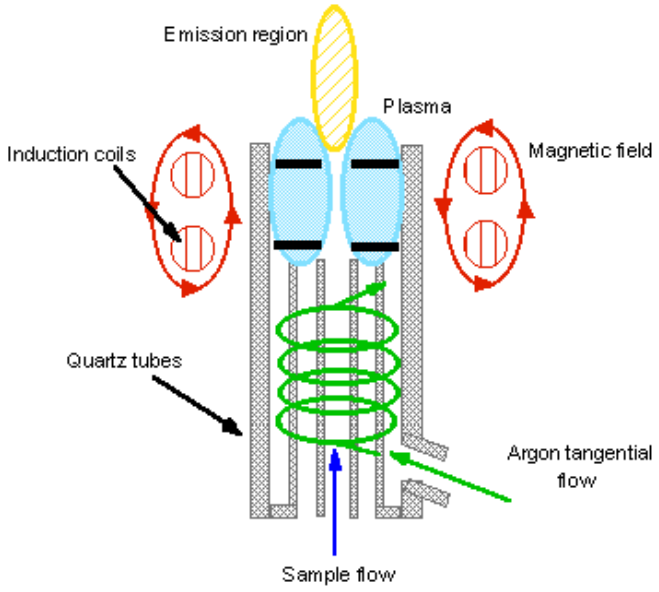

Figure 3. A typical plasma source. Argon gas is passed through a quartz tube and the tip of the quartz tube is surrounded by induction coils that create a magnetic field. The magnetic field excites the pre-seeded electrons which then ionizes the argon atoms. Reversing the magnetic field changes the direction of the excited ios and causes more collisions with argon atoms results in further ionization of the argon atoms and intense thermal energy. As a result, a flame shaped plasma forms on top of the torch. Picture from http://campus.murraystate.edu/academic/faculty/judy.ratliff/page.htm

The samples were read by the Optical Emission Spectrometer (Optima 4300 DV, PerkinElmer Instruments) operated by the software WinLab32™ Instrument Control, v2.2, PerkinElmer Inc. The results were compared as the amount of metal ion released over time and total amount released between different test conditions.

Cell Characterizations

The cell parameters, including viability, morphology, intracellular ATP and release of pro-inflammatory products, NO and IL-1β, were used to assess the response of the cells to the alloys and their released metal ions.

Viability Test

At the end of the 3-day tests, viability of the cells on the surface of the alloys and the control cells were assessed by using the Live/Dead® viability/cytotoxicity test kit (Molecular Probe, Eugene, OR). The Live/Dead® test kit uses two reagents, calcein AM and ethidium homodimers-1 (EthD-1). Live cells are distinguished from the dead cells by the presence of intracellular esterase activity and the integrity of their membrane. Esterase in live cells converts the cell-permeant calcein AM to the green fluorescent calcein (ex/em 495/515 nm). Fluorescent calcein is well retained within live cells. EthD-1 enters cells with damaged membranes and binds to the nucleus and produces a red fluorescence (ex/em 495/635 nm). EthD-1 is excluded by the intact

plasma membrane of live cells. Hence only viable cells will take up calcein and fluoresce green and only dead or dying cells will bind EthD-1 and fluoresce red.

Medium was removed carefully from the corrosion cell and controls. Ca^{2+}-Mg^{2+}-free phosphate buffered solution (PBS) containing 2 mM calcein AM and 4mM EthD-1 was added to the cells and incubated at room temperature for 20-40 minutes. The samples were then covered with glass cover slips and viewed using a Leica® Confocal Laser Microscope. The viability of non-activated and activated macrophage cells on test alloys was qualitatively compared to controls (portions of green color vs. red).

Morphology

Cells undergo morphological changes when activated, injured or even grown on different surfaces. Morphology of the non-activated cells and activated cells on glass (control) and alloy surfaces were observed using scanning electron spectroscopy (SEM). SEM directs high-energy electron beams to the samples. These primary electrons interact with electrons and atoms in the sample and cause the secondary electrons to be emitted from the sample. The secondary electrons are collected by the photoamplifier tube and used to create an image of the samples up to 100,000x. Control cells and cells grown on testing alloys were prepared by washing twice with PBS to remove cell culture medium and fixed with 2.5% glutaldehyde + 0.1 M potassium phosphate solution to crosslink protein to preserve the morphological structure. After 30 minutes, the glutaldehyde solution was removed and cells were rinsed twice with PBS.

The samples were then dehydrated with a series of ethanol solutions (30%, 50%, 70%, 95% and 4 times 100%) for 10-15 mins each concentration. Finally hexamethyldisilazane (HMDS) was added to remove the ethanol. Samples were air-dried (to evaporate HMDS) overnight and stored in a desiccator. Because protein is not conductive, samples were coated with Au-Pd before placing in the vacuum chamber to avoid charge build up on samples. Images of non-activated cells and activated cells on different alloys were compared qualitatively by looking at cell size, cell membrane processes and surface extensions.

ATP

The amount of intracellular ATP was used as an indicator of cell well-being (Bumgardner *et al*. 1995) as well as indicator of cell activation since intracellular ATP concentrations were reported to be approximately 2-3 times higher than that of non-activated macrophage cells (Loike *et al*. 1979). ATP concentrations were determined based on the luciferin/luciferase reaction using the Enliten® ATP assay system (Promega, Madison, WI). The detection range of the kit is $1x10^{-17}$ to $1x10^{-11}$ mole ATP per sample. In the reaction, luciferase catalyzes luciferin to react with oxygen in the presence of one ATP molecule to form Oxyluciferin.

$$ATP + luciferin + O_2 \xrightarrow{luciferase} oxyluciferin + ADP + Pi + h\nu\ (560nm)$$

The byproduct is the emission of a photon at 560 nm (Crouch *et al*. 1993; Lundin 1979) and the number of photons counted using a photo-multiplier tube is directly proportional to the amount of ATP in the sample solution.

At the end of each 3-day test, medium from the corrosion cell and petri dish (control) were carefully removed and rinsed with serum-free medium because proteins in the serum of the medium might interfere with the luciferin-luciferase reaction. Cells were scraped off the surface and resuspended with 1-2 ml of the serum-free medium. The number of cells was counted using a hemocytometor. A 150 µl aliquot of the cell suspension was pippetted into each of the three plastic tubes. One tube at a time was placed in the FB 15 Luminometer (v2.0, Zylux Corp. Maryville, TN). The software (FB 12, Zylux Corp. Maryville, TN) was programmed so that after the door was shut, 100 µl of lysing solution (0.1 M tris-acetate + 4mM EDTA + 0.1% triton x100 at pH 7.75) was added to the tube to lyse the cells and release ATP. After a 0.5 second delay, 80 µl of luciferin/luciferase solution was added to initiate the reaction. The photons were counted and recorded every second for 15 seconds after the last addition and reported as relative light units (RLU). A standard curve was made and showed RLU was proportional to the amount of ATP (mole) released by cells. The number of cells in each test and control wells was used to normalize the amount of ATP to moles/cell. ATP concentrations in non-activated and activated macrophage cells on test alloys were compared to those in the control cells.

Nitric oxide (NO)

NO is a reactive nitrogen species released by macrophage cells during inflammation. It may be a key mediator in inhibiting DNA synthesis, in cell proliferation, and in stimulating Prostaglandin E_2 (PGE_2) (a bone-resorbing and bone-

forming substance produced by osteoblasts) release during inflammatory responses (Shanbhag *et al*. 1998). Nitric oxide has also been known to act on endothelial cells to cause increased local blood flow (Bevilacqua, 1993) to facilitate the delivery of leukocytes to local sites of injury. NO produced by the osteoblasts has been proposed to cause bone resorption by osteoclasts (van't Hof and Ralston, 1997; Riancho *et al.*, 1995).

NO becomes NO_2^- in cell culture conditions, hence the concentration of NO_2^- should increase in proportional to NO release in medium during tests with activated cells. NO was read daily during the 3-day corrosion test with non-activated cells and activated cells. It must be read soon after the supernatant was removed from the corrosion cell because it was a very unstable compound. Supernatant (or deionized water for a blank test) was pipetted into 3 wells (150 µl each) of the 96-well plate, and 130 µl deionized water and 20 µl Griess® reagent (0.5 % of sulfanilic acid + 0.05 % n-(1-naphthyl) ethylenediamine dihydrochloride, Molecular Probes, Eugene, OR) was then added to each well. The plate was then incubated at room temperature for 30 minutes. $NO_2^-{}_{(aq)}$ reacts with sulfanilic acid and is converted to a diazonium salt by reaction with the nitrite (NO_2^-) in the solution. The diazonium salt is then coupled to n-(1-naphthyl)ethylenediamine to form an azo dye that can be read at 548 nm (A_{548}) by a spectrophotometer (µQuant, Bio-Tek Instruments, Inc. Winooski, VT). A_{548} was converted into µM using a standard curve. The detection range of the assay is 1-100 µM. NO released by non-activated and activated macrophage cells on test alloys was

normalized at day 3 to nmole/cell and was compared to that released by the control cells.

IL-1β

Activated macrophages are known to release IL-1β. It acts on fibroblasts to regulate their proliferation and induce vascular endothelial cells to express surface receptors that render these cells more adhesive to leukocytes (Goldring *et al*., 1983; Goldring *et al*., 1986). It may also activate osteoclast and promote bone resorption (Miller and Anderson, 1988; Miller *et al.* 1989). In this study, IL-1β was used to assure activation of cells by the addition of LPS and IFN-γ. It was also used to determine if the presence of metal and metal ions affected the release of IL-1β from non-activated or activated cells. Supernatants collected daily from the 3-day tests were stored at –20^{o}C to prevent IL-1β from degrading and thawed one day prior the analysis. The analysis of IL-1β in the supernatant was conducted using a commercial ELISA kit (Quantikine M, R&D System, MN). The detection range of the kit is 8-500 pg/ml. The assay employs the quantitative sandwich enzyme immunoassay technique. A mouse IL-1β antibody was pre-coated onto a 96-well plate. Fifty μl of assay diluent and 50 μl of test sample were pipetted into each well. Any IL-1β in the test sample binds to the precoated IL-1β antibody. After two hours, the plate was washed five times with the wash buffer to remove medium and diluent. One hundred μl of horseradish peroxidase-linked IL-1β antibody was added to bind to the immobilized IL-1β from the samples. Two hours

later, wells were washed five time with the wash buffer to remove the unbounded enzyme-antibody conjugate. One hundred μl substrate solution (hydrogen peroxide and tetramethylbezidine (chromogen)) was added to the wells so the peroxidase reacted with the hydrogen peroxide for 30 minutes and yielded blue color. It turned yellow after stop solution (100 μl HCl solution) was added. The absorbance at 450 nm (A_{450}) of each sample and the blank (fresh cell culture medium) was read in duplicates The absorbance was proportional to the amount of IL-1β present in the samples. From a standard curve, A_{450} was transferred in to IL-1β concentration in pg/ml. IL-1β released by non-activated and activated macrophage cells on test alloys was normalized to pg/cell and compared to that released by the control cells.

Surface Analysis: X-ray Photoelectron Spectroscopy (XPS)

XPS is a surface analysis technique capable of providing elemental and chemical information on the top 100 Å of the surface. In XPS, x-rays are used to excite electrons from the inner shell of the surface atoms. The emitted electrons are counted (intensity) and their binding energies are calculated by a hemispherical analyzer. Binding energy (eV), BE, equals to the energy of the x-ray subtracted by the kinetic energy of the electron when reaching the analyzer. BE of each electron is unique to each element and can be used to identify elements present on the surface. BE can be affected by the chemical states of each element, e.g. metal oxide, hydroxide, carboxide etc. and small shifts in BE may be used to identify the chemical bonding of the elements on the surface.

Samples of both alloys were cut into approximately 1.0 x 1.0 x 0.1 cm coupons to fit inside XPS for surface analysis. The surfaces of these coupons were prepared identically as before. Coupons were first evaluated as polished with XPS to verify all samples from the same alloy had the same surface composition and peak intensity. By subtracting the spectra from one another, the residual spectra simply represent background noise without major peaks.

The samples were then disinfected with 70% ethanol and UV light and placed in wells of a cell culture plate. Medium, non-activated cells and activated cells were added with the same seeding density to duplicate the conditions imposed on the test samples in the electrochemical corrosion cells. After three days, the coupons were rinsed with deionized water to remove cells and medium. They were then placed into the vacuum chamber (pressure around 10^{-10} torr) of a XPS (Physical Electronics Phi 1600, Eden Prairie, MN) with X-ray power adjusted to 15 kV and 300 W. The samples were positioned at a 45^{o} take-off angle with respect to the analyzer. Survey spectra were averaged from 10 scans with pass energy 46.95 eV and high resolution spectra were averaged from 15 scans with pass energy 23.5 eV.

Survey spectra were used to identify the presence of surface elements and to calculate their composition in atomic percentage. High resolution spectra were used to identify chemical states and changes in chemical states of the surface elements of major surface oxide components. Oxygen peaks from both alloys were deconvoluted and the area under each peak was used to calculate the percentage of metal oxide among all

oxygen species. A software package (Spectral Data Processor v 2.3, XPS international Inc.) was used for the above calculations.

Statistical Analyses

The statistical analyses were done using the Statlets software package (Statlets, v1.1B, NWP Associate Inc.). Two way analysis of variance (ANOVA) based on the factorial design model was used to differentiate between test conditions and over three days (Factors include three conditions and time-day 1, 2, and 3). Statistical differences were declared as $p<0.05$.

CHAPTER III
RESULTS

Corrosion Tests: Three-Day Open Circuit Potential and Direct Current Test

Co-Cr-Mo

Factorial analysis indicated there were no significant interactions between time and conditions for the open circuit potential (OCP) and current measurements ($p<0.05$). The OCP and current transfer of Co-Cr-Mo over 3 days in different conditions are listed in Table 1 and Table 2. The OCPs for Co-Cr-Mo did not show any statistical difference over 3 days. There was a difference in OCP between medium and cells, but they were not different from activated cells. For all conditions, the direct current values on Day 1 were all significantly higher than Day 2 and 3; no difference between day 2 and 3. For all conditions, the current transfer values on Day 1 were all significantly higher than Day 2 and 3; no difference between day 2 and 3.

Table 1. OCPs (mV vs. SCE) of Co-Cr-Mo with medium, non-activated cells and activated cells (n=3). Same letters represent values without a statistically significant difference within the column and across the rows.

	Day 1 (mV vs. SCE)	Day 2 (mV vs. SCE)	Day 3 (mV vs. SCE)
Medium	-344.0±17.1 [a]	-376.7±41.9 [a]	-390.3±52.2 [a]
Cells	-262.0±9.1 [b]	-302.0±26.6 [b]	-300.3±18.9 [b]
Activated Cells	-293.7±81.1 [ab]	-322.7±52.6 [ab]	-331.7±72.3 [ab]

Table 2. Direct current measurement (mC) of Co-Cr-Mo with medium, non-activated cells and activated cells (n=3). Same letters represent values without statistic significance within the column and across the rows.

	Day 1 (mC)	Day 2 (mC)	Day 3 (mC)
Medium	30.1±3.8[a]	13.1±2.3[d]	12.1±2.1[d]
Cells	18.4±2.8[b]	6.4±2.1[e]	5.6±2.0[e]
Activated cells	6.9±2.8[c]	3.4±1.0[f]	3.2±0.6[f]

The charge transfer values of Co-Cr-Mo summed over 3 days (total charge transfer) in three test conditions are shown in Figure 4. The total 3-day charge transfer in the presence of activated cells was the lowest among all three conditions. For Co-Cr-Mo, the total charge transfer was the highest with medium, followed by cells and then activated cells.

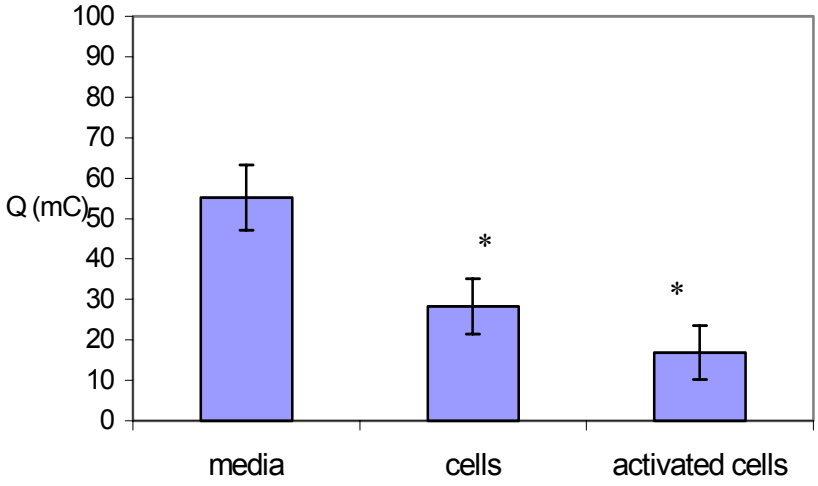

Figure 4. Co-Cr-Mo total charge transfer over 3 days for the three conditions (medium, cells, and activated cells) (n=3). The charge transfer from activated cells was significantly lower than that from medium and non-activated cells ($p<0.05$). The charge transfer from cells was significantly lower than that from medium ($p<0.05$). * indicates statistical difference.

Ti-6Al-4V

Factorial analysis indicated there were no significant interactions between time and conditions for the OCPs and charge transfer for Ti-6Al-4V alloy. OCP values and direct currents over three days are listed in Table 3 and Table 4. For Ti-6Al-4V, the OCP became more electropositive from day 1 to day 2 ($p<0.05$), but not from day 2 to day 3. There was a difference in OCPs between medium and cells ($p<0.05$), but they were not different from activated cells. For the current transferred, values on Day 1 are all significantly higher than Day 2 and 3 for all conditions ($p<0.05$); no difference between day 2 and 3.

Table 3. OCPs (mV vs. SCE) of Ti-6Al-4V with medium, non-activated cells and activated cells (n=3). Same letters represent values without statistic significance within the column and across the rows

	Day 1 (mV vs. SCE)	Day 2 (mV vs. SCE)	Day 3 (mV vs. SCE)
Medium	-505.7±17.9[a]	-283.3±26.0[c]	-247.0±36.5[c]
Cells	-359.5±99.2[b]	-204.8±65.3[c]	-184.5±66.2[c]
Activated cells	-378.6±83.9[b]	-249.4±51.0[c]	-226.0±42.1[c]

Table 4. Direct current measurement (mC) of Ti-6Al-4V with medium, non-activated cells and activated cells (n=3). Same letters represent values without statistic significance within the column and across the rows

	Day 1 (mC)	Day 2 (mC)	Day 3 (mC)
Medium	49.3±13.7[a]	7.4±2.6[c]	5.7±2.0[c]
Cells	61.7±16.3[a]	9.7±2.4[c]	3.8±3.3[c]
Activated cells	19.0±5.3[b]	7.3±2.6[c]	5.4±2.2[c]

The sum of corrosion current (total charge transfer) Ti-6Al-4V over 3 days are shown in Figure 5. The total 3-day charge transfer in the presence of activated cells was the lowest among all three conditions. For Ti-6Al-4V, there was no difference between medium and cells but both these conditions generated higher total charge than with activated cells.

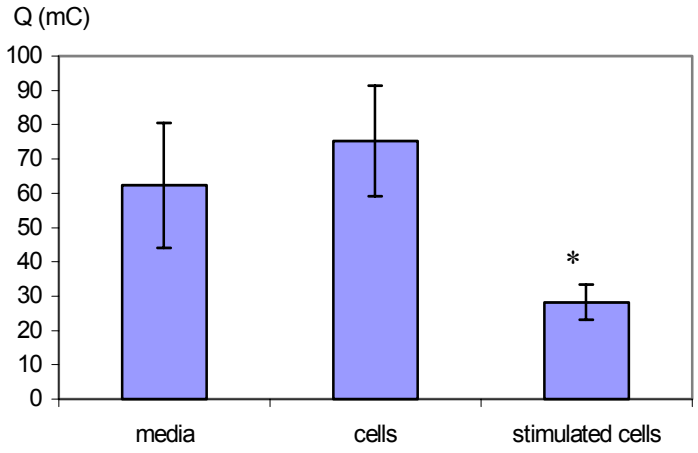

Figure 5. Ti-6Al-4V total charge transfer over 3 days for the 3 conditions (medium, with non-activated cells and activated cells) (n=3). The charge transfer from activated cells was significantly lower than that from medium and cells ($p<0.05$).

Cell Responses on Metal Alloys

Live/Dead and Morphology

Live/Dead

Representative images from the confocal scope, including non-activated cells and activated cells on glass, Co-Cr-Mo and Ti-6Al-4V alloys are shown in Figure 6. Non-activated cells in general exhibited higher cell density on the alloy surface compared to LPS+IFN-γ activated cells. The majority of the cells (both activated and not activated) fluoresced green, indicating cells attached to the plates were viable.

Morphology

The morphology of non-activated cells and activated cells on test alloys and glass controls is shown in Figure 7. The scale bars are located on the lower left corner of the pictures.

After three days, non-activated cells formed a monolayer on the surfaces of the glass and test alloys and multi-layers in some areas (Figure 7 A, C and E). Activated cells after 3 days were more sparsely distributed on the alloys and glass surfaces (Figure 7 B, D, F and G). Non-activated cells exhibited regular globular shape with few surface extensions on them and more membrane process attaching to the substrate compared to the activated cells. The activated cells were more spindle shaped and had more surface extensions on them and less membrane processes attaching to the substrate compared to the non-activated cells.

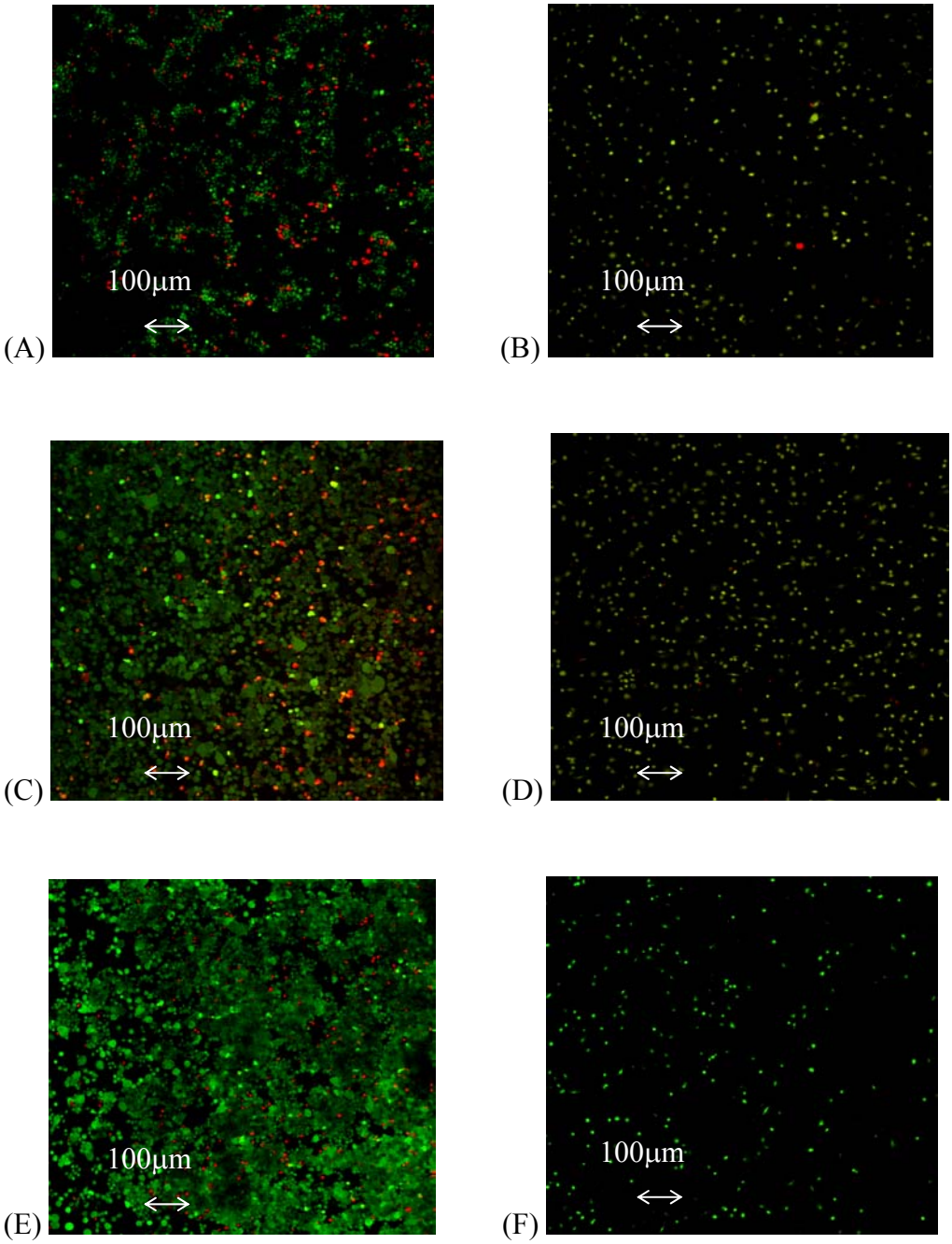

Figure 6. Confocal images from Live/Dead viability tests. (A) TIB cells on glass; (B) LPS+IFN-γ activated TIB cells on glass;(C) TIB cells on Co-Cr-Mo; (D) LPS+IFN-γ activated cells on Co-Cr-Mo; (E) TIB cells on Ti-6Al-4V; (F) LPS+IFN-γ activated TIB cells on Ti-6Al-4V. Green cells were viable and red cells were not viable.

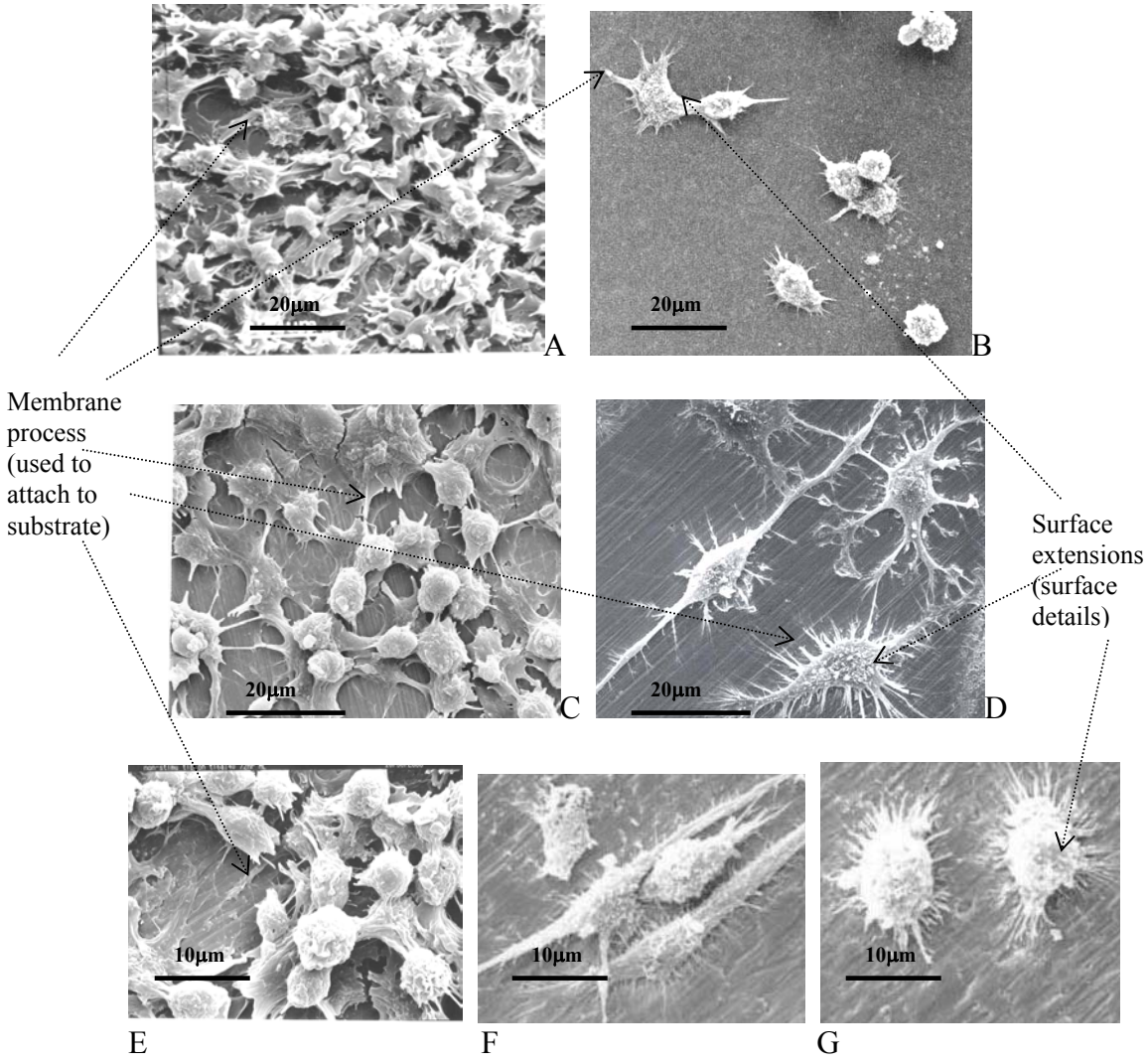

Figure 7. Non-activated (A) and LPS+IFN-γ activated (B) TIB cells on glass (petri dish); Non-activated (C) and LPS+IFN-γ activated (D) TIB cells on Co-Cr-Mo; Non-activated (E) and LPS+IFN-γ activated (F,G) TIB cells on Ti-6Al-4V. After 3 days, non-activated cells formed a mono-layer on the surfaces of the glass and test alloys and multi-layers in some areas (Figure 7 A, C and E). They exhibited regular globular shape with few surface extensions. Activated cells were sparsely distributed on the alloys and glass surfaces (Figure 7 B, D, F and G). They were more spindle shaped and had more surface extensions than the non-activated cells.

Intracellular ATP and Proliferation (Cell Count)

Cell count

At the end of each test, the number of cells was counted using a hemocytometor and the numbers of cells were used to normalize the release of the chemical compounds such as NO and IL-1β on day 3 as well as intracellular ATP. Figure 8 shows the cell numbers counted from controls and the different test conditions with the different test metals.

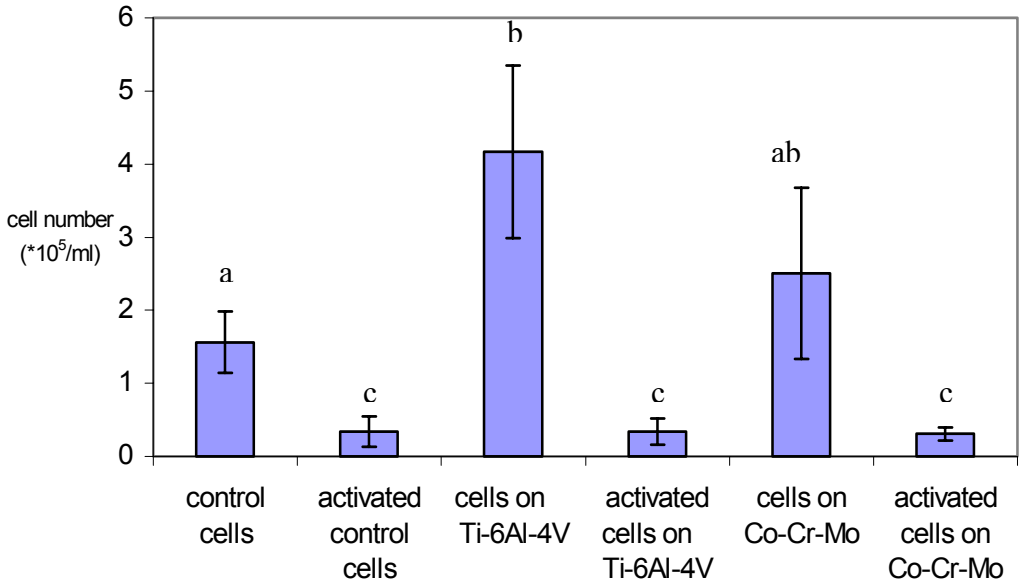

Figure 8. The number of TIB cells and LPS+IFN-γ activated TIB cells in controls and on the test alloys after 3 days. Control: cells grown on glass petri dishes.

Non-activated cells grew up to 4 times the initial seeding population after three days. Cell numbers were higher on the Ti alloy compared to the control ($p<0.05$). There were no statistical differences between the cell numbers on Ti-6Al-4V and Co-Cr-Mo alloys.

Activated cells did not proliferate after seeding; the numbers of activated cells were statistically lower ($p<0.05$) than those of non-activated cells grown on all surfaces. There was no statistical difference of cell numbers between test alloys and glass.

iATP

The results from the ATP test are shown in Figure 9. Due to the large standard deviations, ATP concentrations were not significantly different between non-activated cells and activated cells; nor were there differences between the two metals and the control.

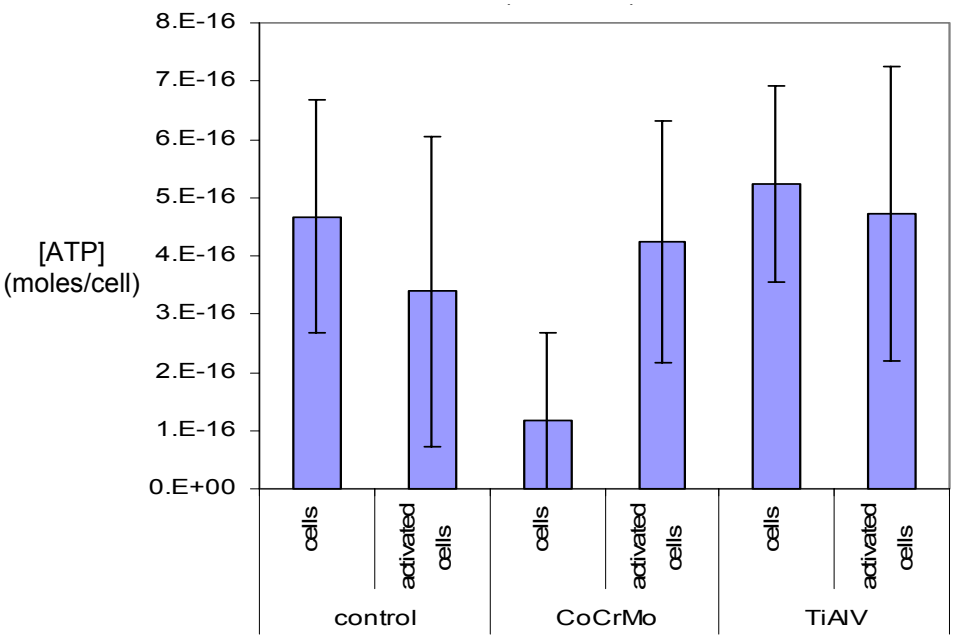

Figure 9 ATP concentrations (moles/cell) at the end of the 3-day test. Control: on glass petri dish. Non-activated TIB cells and LPS+IFN-γ activated cells did not show differences in ATP concentrations for all conditions.

Release of Cellular Chemicals

Nitric oxide (NO) concentrations

Tables 5 and 6 list the concentrations of NO (μM) measured from non-activated cells and activated cells cultured on glass, Co-Cr-Mo and Ti-6Al-4V surfaces daily. The numbers were not normalized to each cell since cell numbers were not counted on day 1 and day 2. For both the alloys, non-activated cells did not release appreciable concentrations of NO on the glass and on the metal surfaces, and activated cells release significaly higher concentrations of NO than non-activated cells. The NO concentration in the supernatant with activated cells increased over 3 days and there was no difference in NO release between the controls and the metal groups for both alloys. Non-activated cells on Ti-6Al-4V released more NO than those on glass. No cross effects were found between time (3 days) and treatments (conditions) ($p<0.05$).

Table 5. The nitric oxide concentrations (μM) from cells cultured on Co-Cr-Mo.

		Day 1 (μM)	Day 2 (μM)	Day 3 (μM)
Cells	**Glass**	0.45±0.64	0.51±0.43	1.87±1.43
	Co-Cr-Mo	1.33±4.37	3.98±2.04	4.43±3.88
LPS+IFN-γ	**Glass**	6.73±1.30	14.37±4.24	14.86±3.75
Activated cells	**Co-Cr-Mo**	7.24±2.80	15.40±5.41	18.13±4.85

Table 6. The nitric oxide concentrations (μM) from cells cultured on Ti-6Al-4V. *: significant difference.

		Day 1 (μM)	Day 2 (μM)	Day 3 (μM)
Cells	**Control**	0.11±0.10	0.72±0.4	0.97±0.59
	On metal	4.52±0.15 *	2.52±2.2	2.26±1.73
LPS+IFN-γ Activated cells	**Control**	8.95±3.01	13.74±1.84	19.94±3.32
	On metal	6.63±2.86	13.62±4.30	14.66±4.44

On day 3, NO release was normalized to number of cells. The data is shown in Figure 10. There was basically no NO measured from non-activated cells under all conditions. For activated cells, they released NO at 5 x 10^{-4} nmole/cell concentration, and there was no difference between the three test conditions.

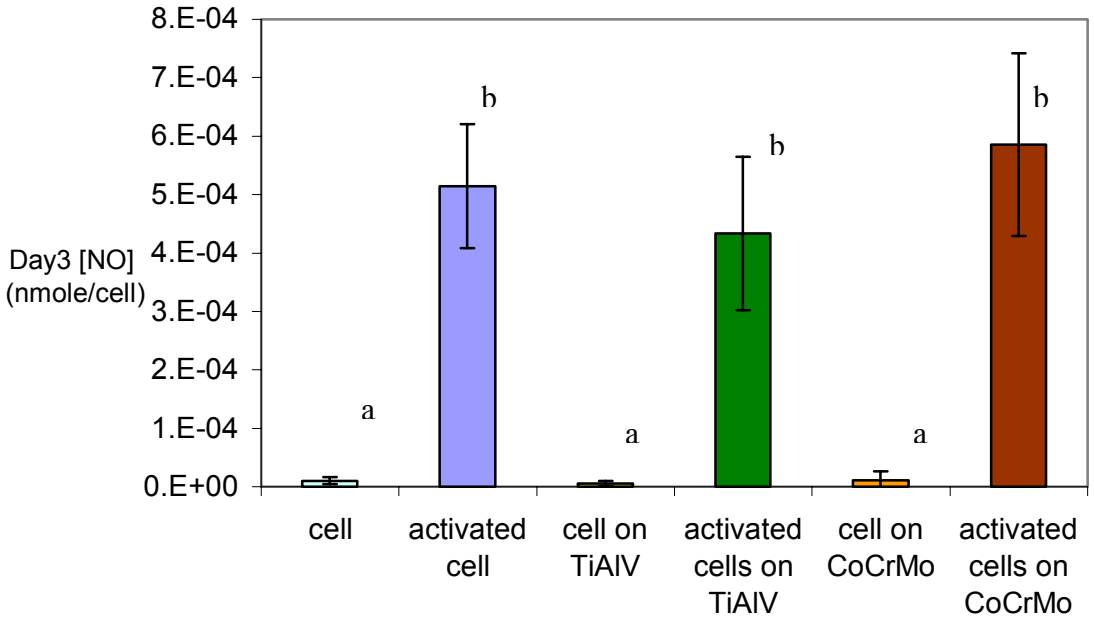

Figure 10. Amount of NO released (nmole/cell) from TIB cells and LPS+IFN-γ activated TIB cells grown on glass, Ti-6Al-4V and Co-Cr-Mo surfaces after three days in culture.

IL-1β

Figure 11 shows the concentrations of IL-1β (pg/ml) measured from each condition daily. The numbers were not normalized to each cell since cell numbers were not counted on day 1 and day 2. There was no IL-1β detected in the supernatant with just non-activated cells except there was a slight increase when cultured with Ti-6Al-4V. With activated cells grown on controls and alloys surfaces, the IL-1β concentrations in the supernatant increased over three days.

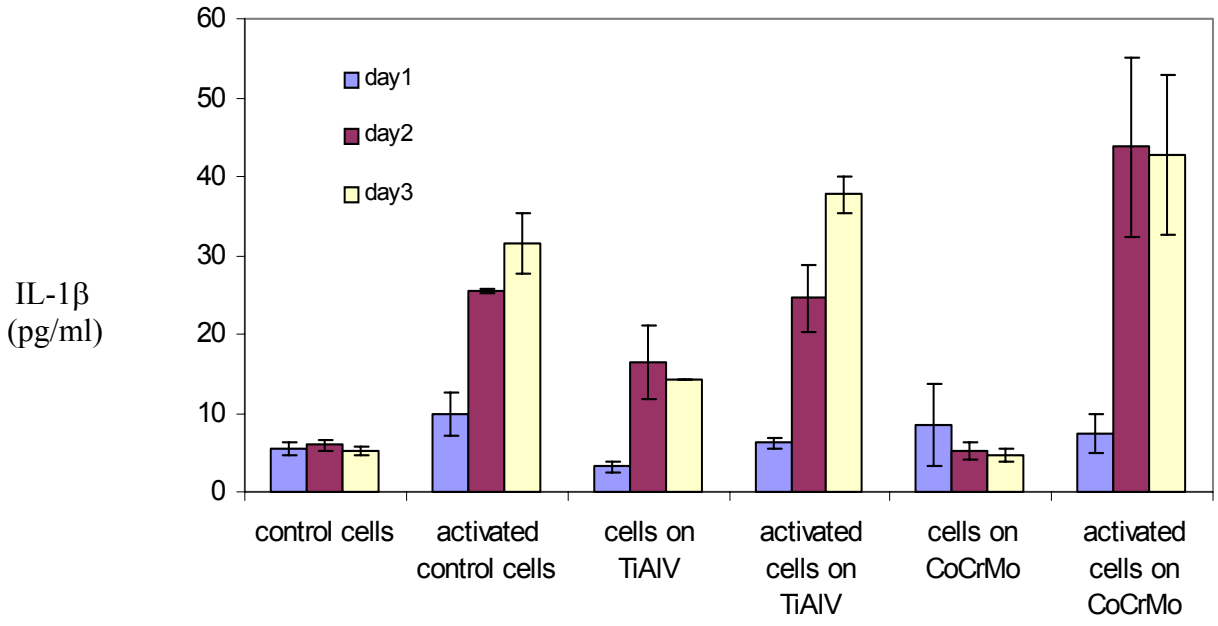

Figure 11. IL-1β averaged concentration (pg/ml) at each day for all conditions.

IL-1β concentrations normalized to the cells numbers (pg/cell) on day 3 are shown in Figure 12. There was essentially no IL-1β measured from non-activated cells under all conditions. Activated cells released IL-1β at 1.2 x 10^{-3} pg/cell concentration.

There was no statistical difference between testing conditions although the IL-1β concentrations appeared to be higher for activated cells on the metals as compared to the controls.

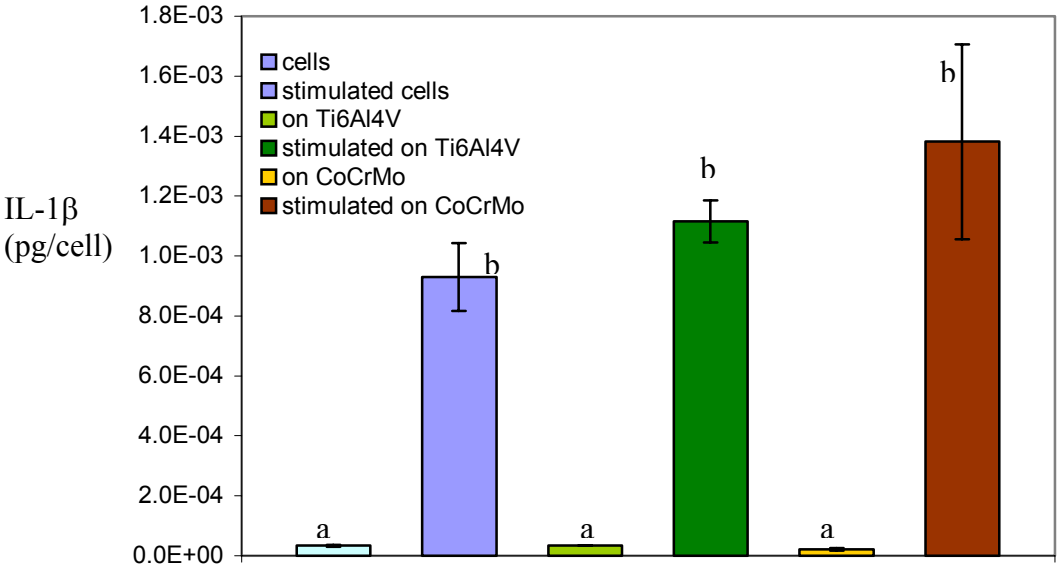

Figure 12. Normalized IL-1β (pg/cell) on day 3 for all test conditions. There was essentially no IL-1β measured from non-activated cells under all conditions. Activated cells released IL-1β at 1.2 x 10^{-3} pg/cell concentration. There was no statistical difference between testing conditions although the IL-1β concentrations appeared to be higher for activated cells on the metals as compared to the controls.

Surface Analysis (XPS)

Figure 13 has the representative curves of the residual spectra from each alloy. Residual spectra were obtained by subtracting survey spectra from each other (within same alloy in as-polished state). This procedure allows for the identification of peaks that are different between individual samples. The residual spectra obtained were simply low intersity noises without major peaks, indicating surface peaks were the same for each as-polished alloy.

Co-Cr-Mo

Representative survey spectra from Co-Cr-Mo alloy after 3 days exposure to medium, non-activated cells and activated cells are shown in Figure 14. The peaks on the as-polished Co-Cr-Mo were carbon (C1s), oxygen (O1s), cobalt (Co3p), chromium (Cr2p) and molybdenum (Mo3d). C1s and O1s appeared on almost all surfaces exposed to atmosphere. Occasionally a silicon (Si2p) peak was identified in the alloy surface composition, and was attributed to the SiC sandpaper used in the sample preparation process. After culturing with medium, most of the peaks in the as-polished spectra decreased in intensity. Generally the intensity of the peaks increased again after culturing with cells, especially with activated cells. This was seen in more detail in the high resolution spectra (Figure 15 a (O1s) and b (Cr2p)). The increase in peak intensity after culturing with cells or activated cells though was variable (Figure 15 c and d).

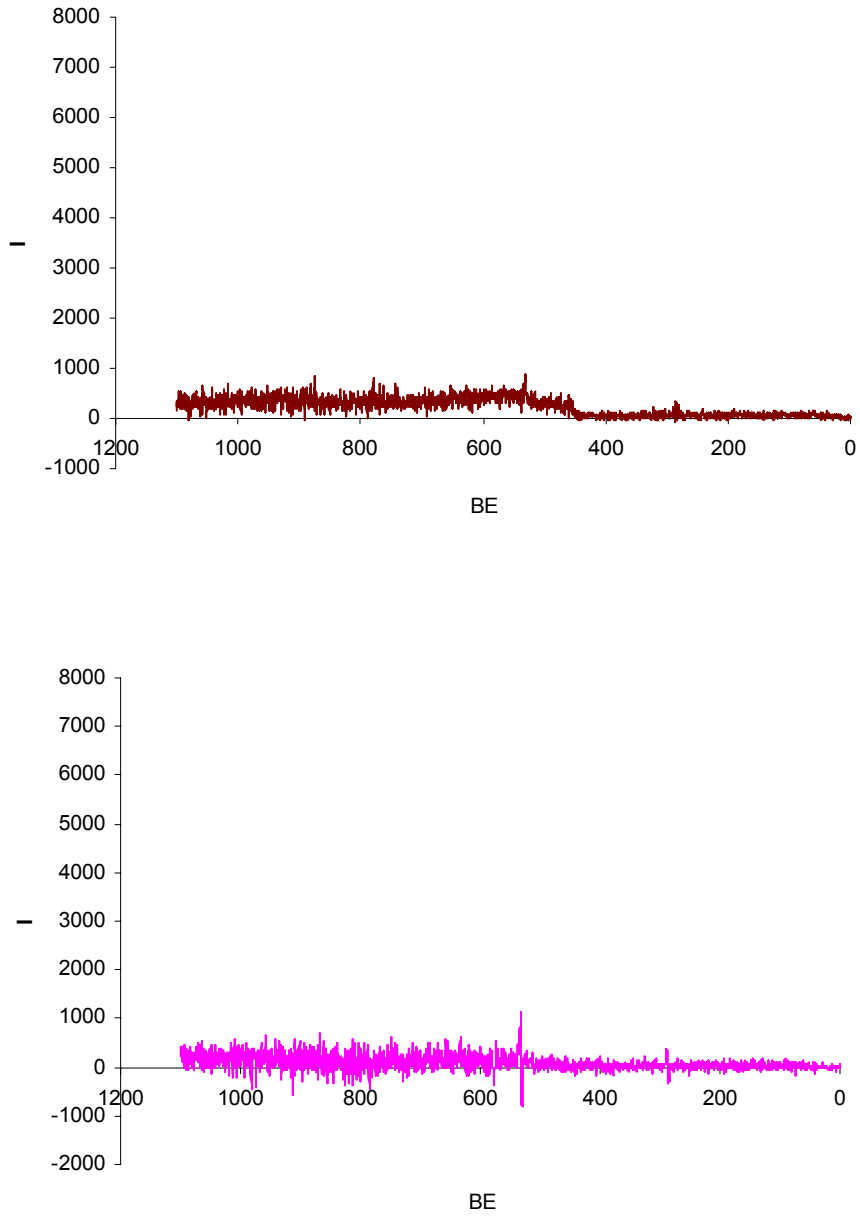

Figure 13. Representative residual XPS survey spectra from as-polished Ti-6Al-4V (top) and Co-Cr-Mo (bottom).The residual spectra used to compare the as-polished surfaces were simply noise. All of the as-polished surfaces of both alloys were concluded identical. BR: binding energy, I: arbitrary intensity.

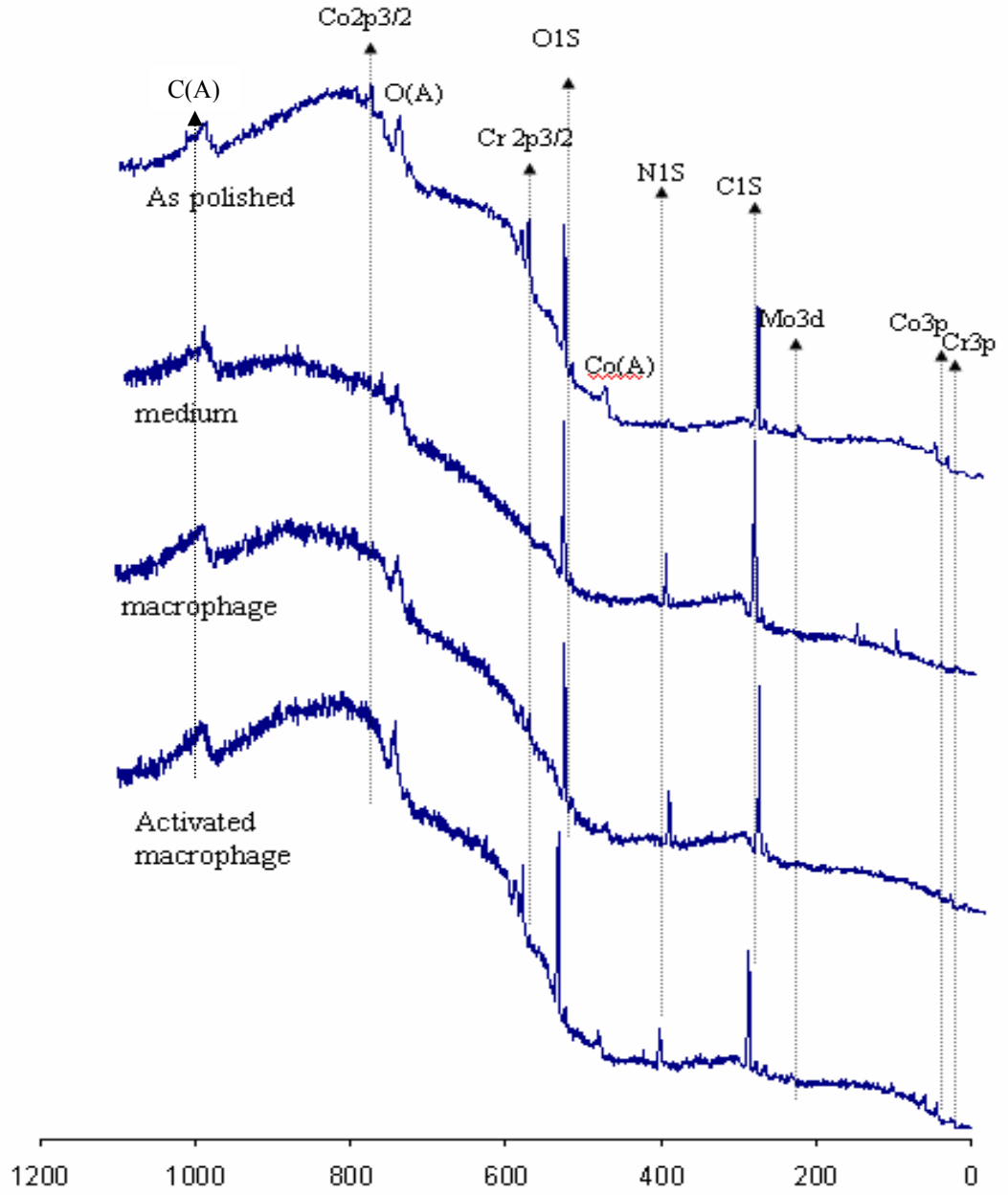

Figure 14. Representative survey spectra from as-polished Co-Cr-Mo and after 3 days exposed to cell culture medium, TIB cells and LPS+IFN-γ activated TIB cells. x: binding energy (eV), y: arbitrary intensity (-). (A): Auger peak.

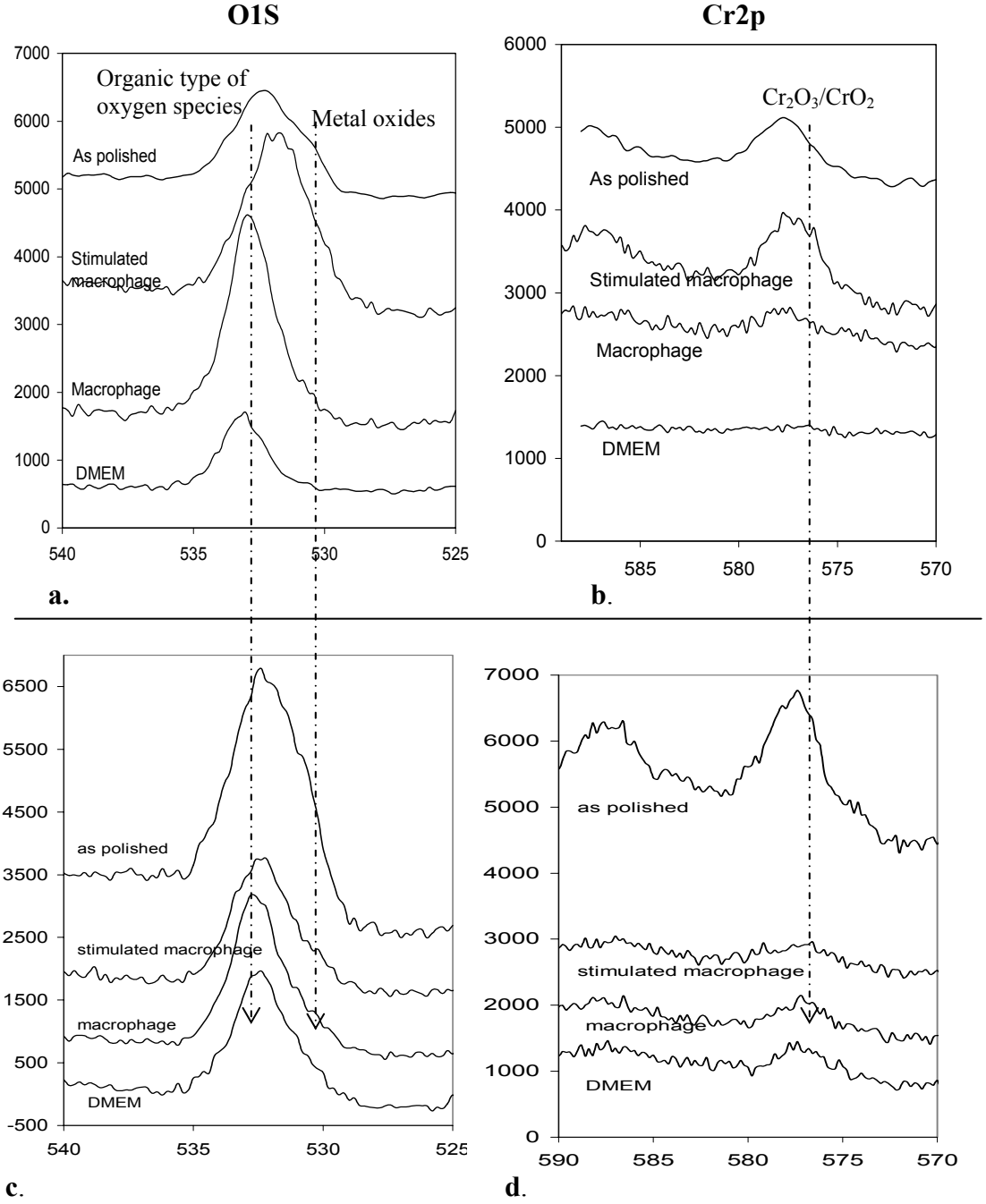

Figure 15. Examples of the high resolution spectra of as-polished Co-Cr-Mo and after 3 days exposed to cell culture medium, TIB cells and LPS+IFN-γ activated TIB cells. a and b, peaks changed with culture conditions; c and d: peaks did not vary with culture conditions. x: binding energy (eV), y: arbitrary intensity (-). Left: O1s peaks, right: Cr2p peak.

By using the Spectral Data Processor v 2.3 software, the percentage of each element present on the surface from the survey spectra was calculated. The percentage of the oxygen (O1s) and chromium (Cr2p) peaks were averaged and the results are shown in the Figure 16.

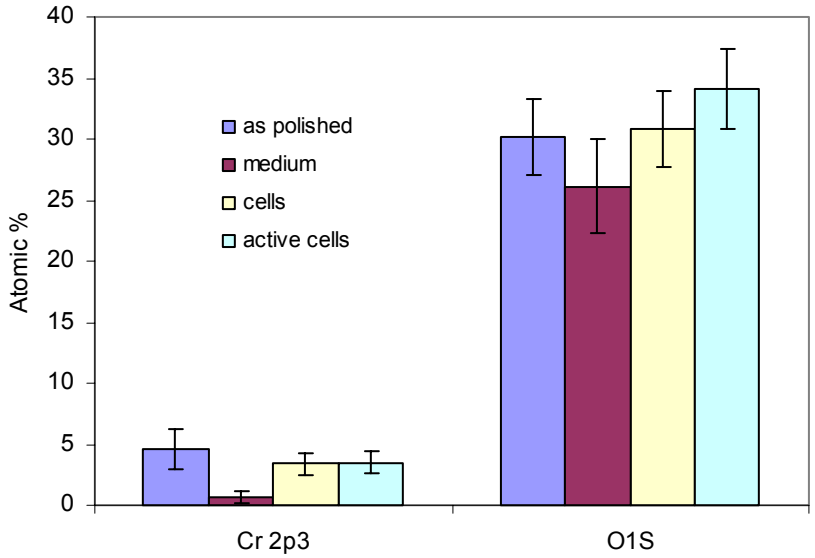

Figure 16. Atomic percentage from the survey spectra. Cr and O on the surface of as-polished Co-Cr-Mo and after culturing with medium, non-activated cells and activated cells. Both atomic percentages of Cr and O decreased with medium (only with Cr $p<0.05$) compared to as-polished surfaces; increased with LPS+IFN-γ activated cells ($p<0.05$) compared with medium.

The average intensity of both oxygen and chromium peaks decreased with medium and increased with non-activated cells and activated cells. Compared to culturing with medium, the peak intensity of both O and Cr increased significantly with activated cells.

To find out the number of the oxygen species present as well as to quantify the percentage of oxygen bound to the metal (metal oxide) on the surface, O1s peaks were fitted using the Spectral Data Processor software. The fitting process stopped when Chi-square stopped changing. The fitting of peaks was specified to have a fixed full width half max (FWHM) =1.6 because of the resolution of the instrument. Three subpeaks with fixed FWHM=1.6 gave the best fitting results for O1s with chi-square approximately 2. Figure 17 is a representative curve of an O1s peak fitted with the three subpeaks.

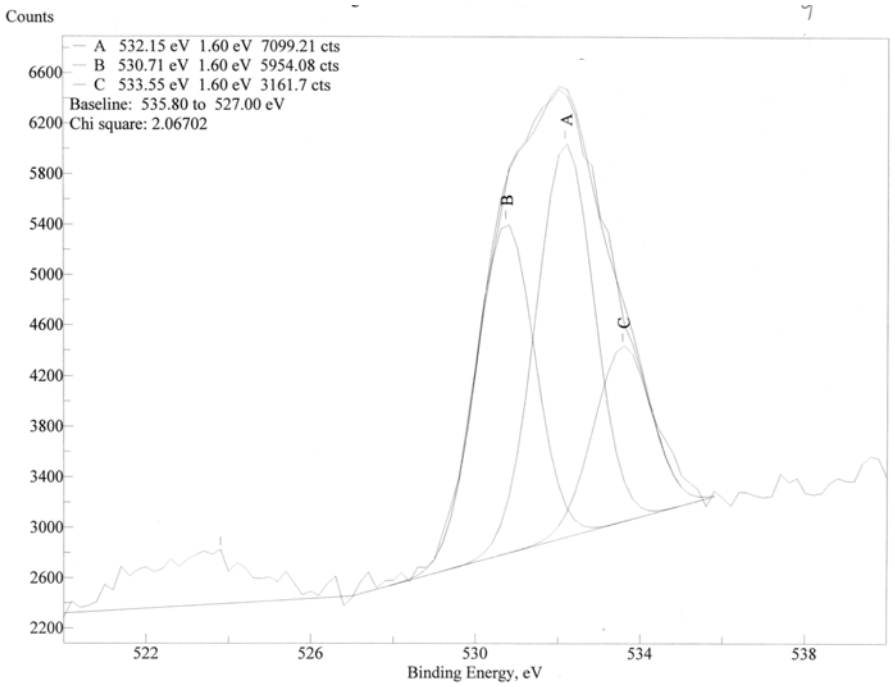

Figure 17. O1s peak of as-polished Co-Cr-Mo fit with three subpeaks (A, B and C). The peak binding energy and chi-square are listed on the left corner. The percentage of area of each peak was calculated and indicated on top of each peak. The peak with lowest binding energy (B) belonged to the metal bound oxygen. The rest of the other two peaks (A and C) were the organic types of oxygen.

The organic types of oxygen (for examples C-O, H-O etc.) had binding energies (BE) around 532-533 eV and the metal-bound oxygens had BE's at ~530 eV. The area under each peak was then calculated and transformed into percentage of the total oxides. The peak at the binding energy near 530 was taken as the part of O bound to the metal atoms and the rest were attributed to organic species. The averaged metal oxide percentage (among all the oxygen species) is shown in Figure 18. The result did not show a statistical difference in changes of the metal oxide percentage between different culture conditions but they were all significantly ($p<0.05$) lower than that of as-polished surfaces.

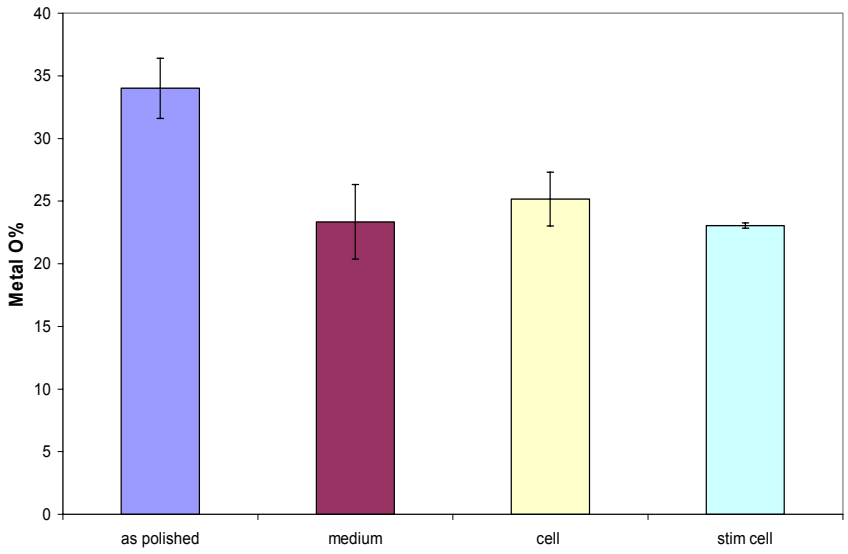

Figure 18. Metal oxide percentage on Co-Cr-Mo from each test condition. No statistical difference in changes of the metal oxide percentage between different culture conditions but they were all significantly ($p<0.05$) lower than that of as-polished surfaces.

The BE of Cr peak in this study was at ~576.6 eV, which is the BE of Cr as in Cr(III) and/or Cr(IV) form (Cr_2O_3 and/or CrO_2 compounds). Co2p and Mo3d were identified only on as-polished sample surfaces. They were not identified on surfaces after 3 days culturing with medium, non-activated cells and activated cells.

The nitrogen peak (N1s) was also fitted with the software and only one type of nitrogen species was found present on the surfaces (medium, non-activated cells and activated cells). Often nitrogen peak was not observed on the as-polished and passivated surfaces; even if was, the peak intensity was fairly small (<50 unit). The nitrogen was at BE~ 401 eV, which corresponds to N-H, C-N types of compounds. No signs of nitrite (~404-405 eV), nitrate (~407-408 eV) and metal nitrides (~396.5-397.4 eV) were found on any surface.

Ti-6Al-4V

Figure 19 is the survey spectra from Ti-6Al-4V after 3 days exposure to medium, non-activated cells and activated cells. The major peaks identified on the as-polished Ti-6Al-4V were carbon (C1s), oxygen (O1s), titanium (Ti2p) and vanadium (V3p).

As seen in Figure 20, after culturing with medium, all the major metal peaks almost disappeared. The peaks reappeared (or increased in intensity) after culturing with cells, especially with activated cells. From the binding energy of the oxygen peak, it was purely the organic type of oxygen (~532-533eV) on the surface when cultured with medium. After cells and especially stimulated cells were cultured on the surface,

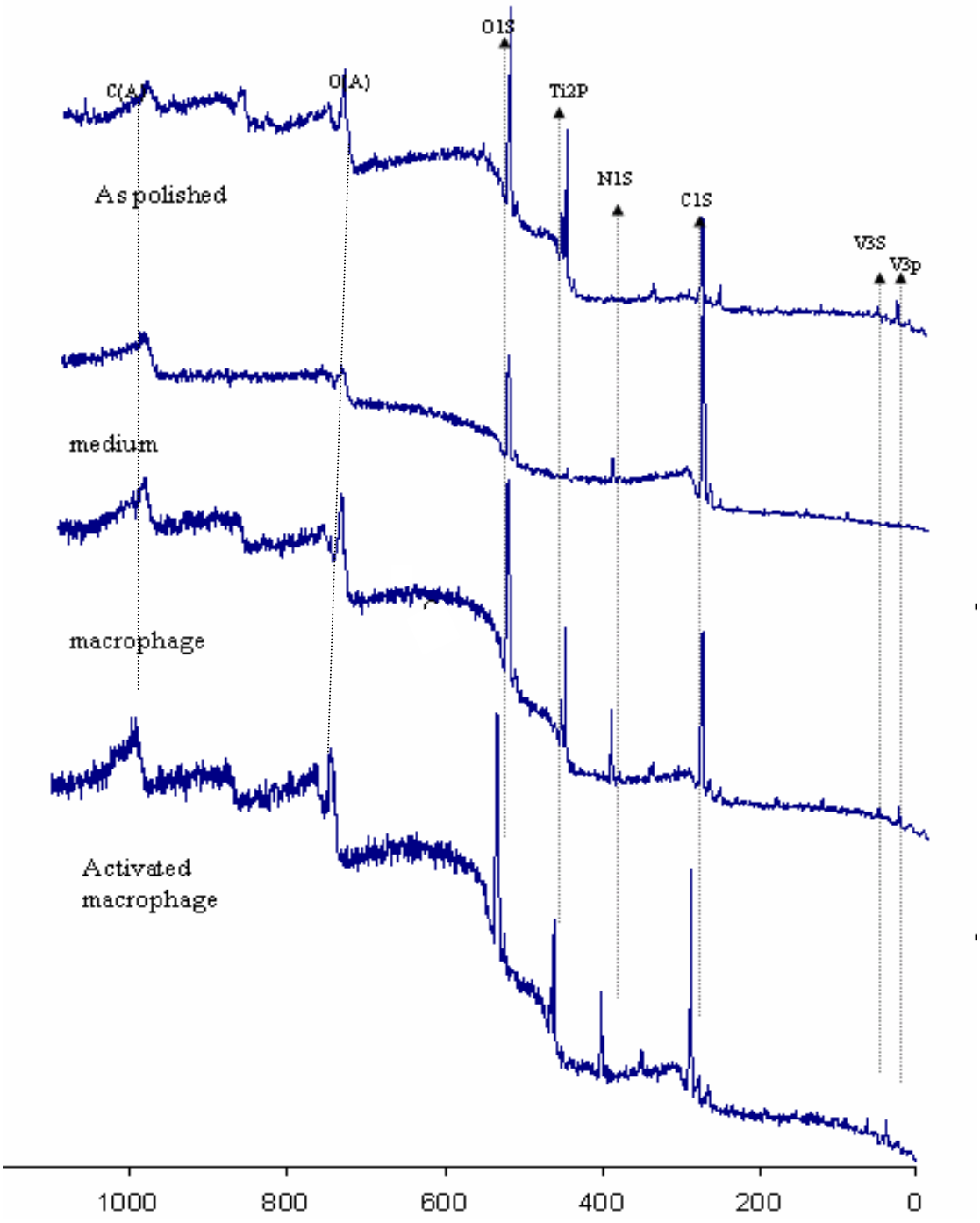

Figure 19. Examples of survey spectra from as-polished Ti-6Al-4V and it with medium, TIB cells and LPS+IFN-γ activated TIB cells after three days. x: binding energy (eV), y: arbitrary intensity (-). (A): Auger peak.

the O1s binding energy shifted toward the metal oxides (~530 eV), which indicated an increase in metal oxide on the surface. It could also be seen that the intensity of Ti peak increased after non-activated cells and activated cells were present. The binding energy of Ti was ~458.6 eV, indicated that the Ti had a chemical state of Ti (IV) and the oxide was mostly composed of TiO_2.

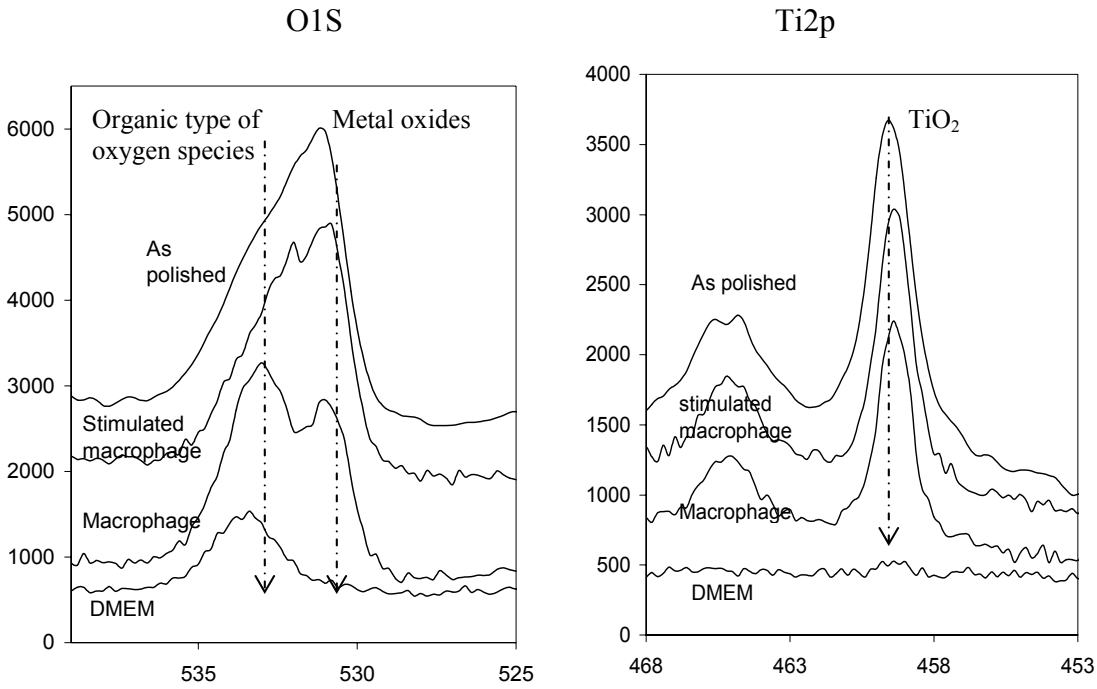

Figure 20. Examples of the high resolution spectra of as-polished Ti-6Al-4V cultured with medium, TIB cells and LPS+IFN-γ activated TIB cells after three days. x: binding energy (eV), y: arbitrary intensity (-).Left: O1s peaks, right: Ti2p peak.

The atomic percentage of each element present on the surface of Ti-6Al-4V was calculated from the survey spectra. The atomic percentage of the oxygen (O1s) and

titanium (Ti2p) peaks were averaged, and the results are shown in Figure 21. The average intensity decreased with medium and cells and increased with activated cells. These changes in the oxygen and titanium peaks were statistically significant ($p<0.05$).

The O1s peaks were fitted using the same procedures as with the Co-Cr-Mo alloy. The χ^2 values were around 2-2.5 after fitting. The averaged percentage of the metal oxide is shown in Figure 22.

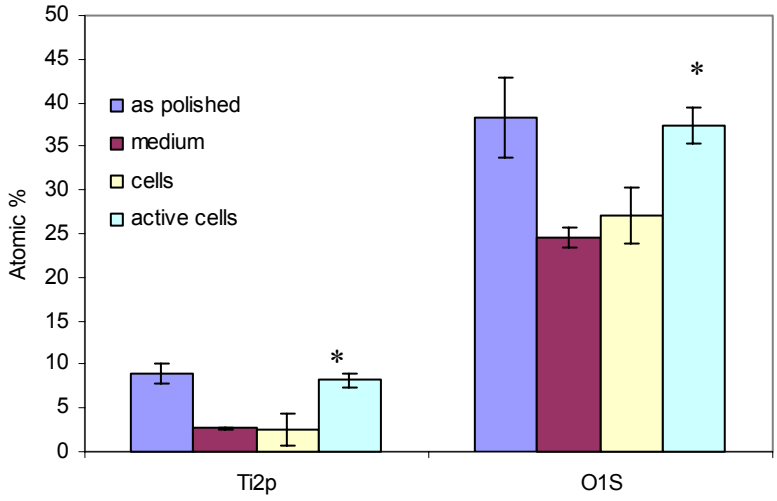

Figure 21. Atomic percentage of Ti and O on the surface of as-polished Ti-6Al-4V and after culturing with medium, non-activated cells and activated cells. Atomic percentage with activated cells was significantly higher compared to medium and cells ($p<0.05$).

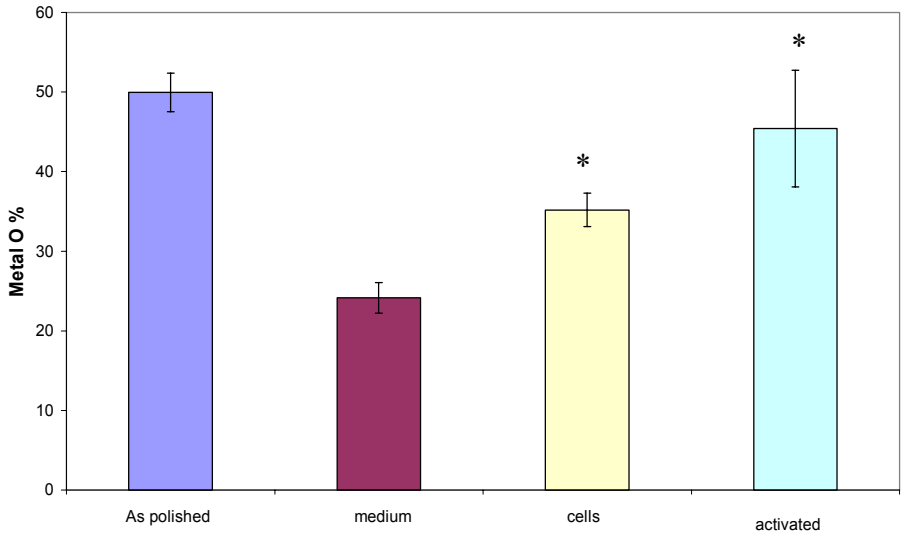

Figure 22. Ti-6Al-4V metal oxide percentage on as-polished surfaces, with medium, non-activated cells and activated cells. Media had lowest metal oxide of all test conditions. The increment with non-activated cells and activated cells was all significant compared to each other. The activated cells had similar metal oxide to the as-polished surfaces.

Compared to the as-polished metal percentage, the metal oxide on the surface with medium decreased almost by half. It increased significantly after culturing with the cells and reached the same percentage as the as-polished surface when cultured with activated cells. All the differences were statistically different ($p<0.05$).

Ion release (ICP-AES)

Co-Cr-Mo

The data on the ion release from Co-Cr-Mo was plotted as concentration (ppb) for each day for each test condition (Figure 23). The sum of total metal ion release under each condition was plotted as well in Figure 24.

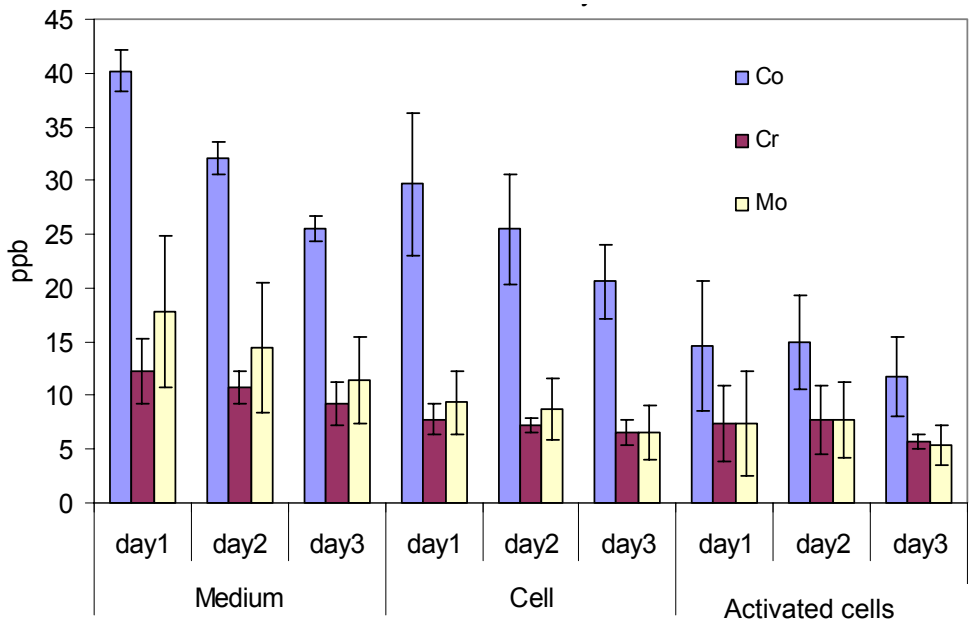

Figure 23. Amount of metal ions released from Co-Cr-Mo (ASTM F75) over 3 days incubated with cell culture medium, macrophage cells and activated macrophage cells.

The release of Co ion was the highest of all the metal ions measured ($p<0.05$). When cultured with medium and cells, its concentration decreased over 3 days ($p<0.05$). While with activated cells, it stayed low and did not vary over time. The concentrations of the other ions (Cr and Mo) were lower than that of Co and did not vary statistically over time.

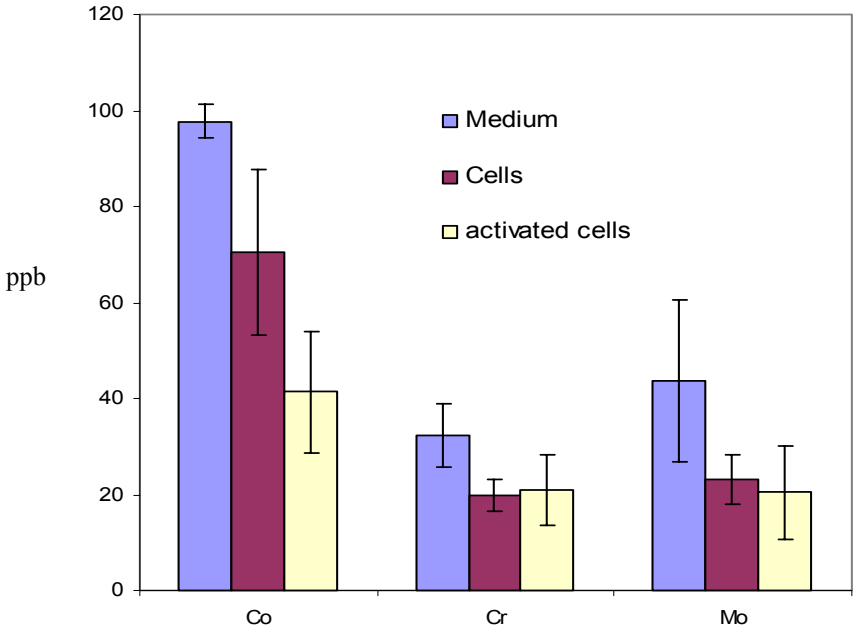

Figure 24. The Co, Cr and Mo total ion release (sum of three days) under each test condition. [Co](medium)>[Co](cells)>[Co](activated cells) ($p<0.05$). [Cr](medium)>[Cr](cells)=[Cr](activated cells). [Mo](medium)>[Mo](cells)= Mo](activated cells). [ ]: concentration in ppb; >: statistically higher ($p<0.05$); =: statistically not different ($p>0.05$).

The total ion release under each condition showed that samples cultured with activated cells release significantly less amount of Co ions compared to those with cells and medium. Even just with cells, Co release was lower than with medium. As for Cr and Mo, non-activated cells and activated cells cultured samples released significantly less ions compared to that with medium. There was no difference in Cr and Mo ion release between cells and medium.

Ti-6Al-4V

The data on the ion release from Ti-6Al-4V was plotted as concentration (ppb) each day for each ion in Figure 25. The sum of total ion release under each condition was plotted as well in Figure 26.

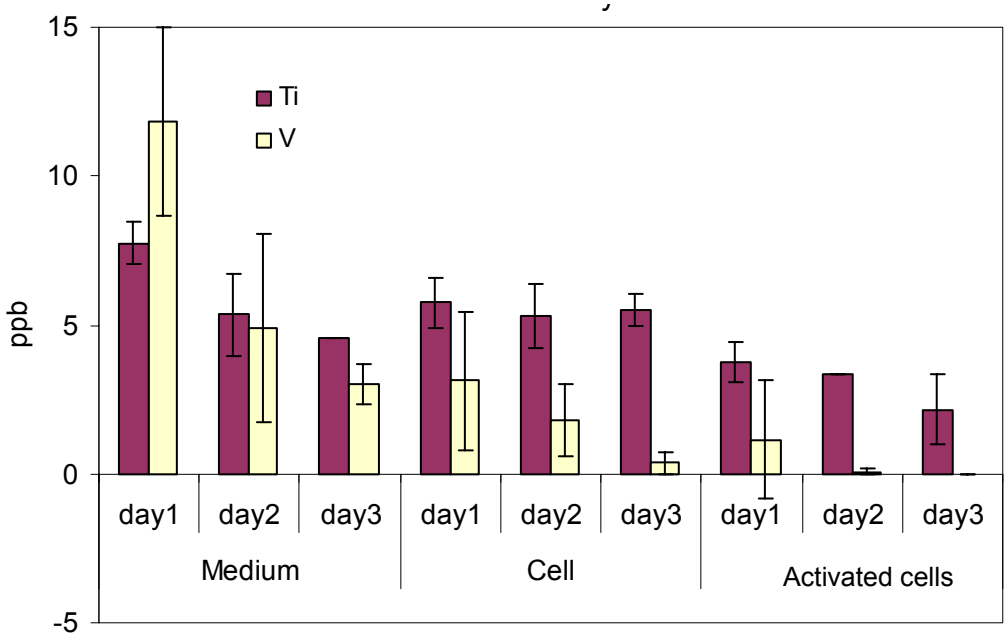

Figure 25. Amount of metal ions released from Ti-6Al-4V (ASTM F136) over 3 days incubated with cell culture medium, macrophage cells and activated macrophage cells.

Because of the high Al background (~50-60 ppb), the change of the Al ion could not be distinguished and thus was not displayed on the graph. The Ti ion decreased over 3 days with medium ($p<0.05$) but remained almost the same with non-activated cells and activated cells. As for V ion release, it decreased over 3 days with medium ($p<0.05$) but did not vary significantly over time with non-activated cells and activated cells.

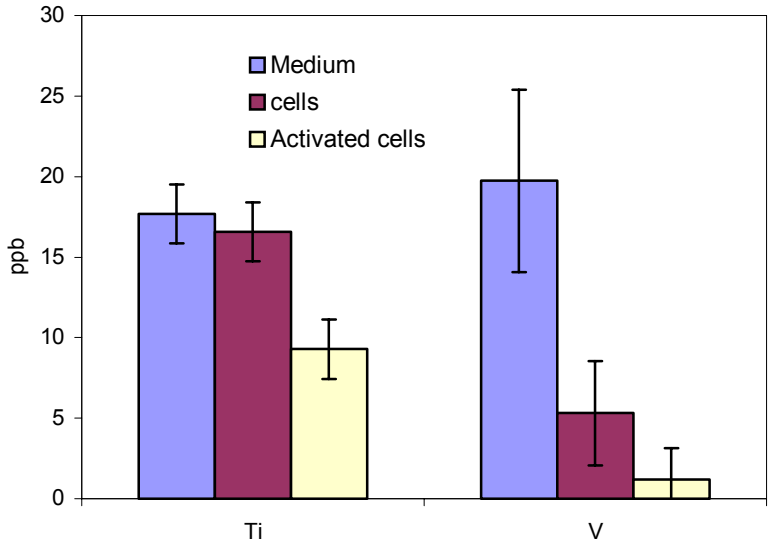

Figure 26. The Ti and V total ion release under each condition. [Ti](medium) = [Ti](cells) > [Ti](activated cells) ($p<0.05$). [V](medium) > [V] (cells) = [V](activated cells). [ ]: concentration in ppb; >: statistically higher ($p<0.05$); =: statistically not different ($p>0.05$).

The total ion release for both Ti and V was the lowest when the metals were cultured with activated cells ($p<0.05$). With medium, Ti and V released similar amount of ions. With non-activated cells and activated cells, less V ion was released ($p<0.05$) compared to Ti.

CHAPTER IV
DISCUSSION

The Co-Cr-Mo and Ti-6Al-4V alloys are known for their corrosion resistance and mechanical strength. They are used in the medical industry as total hip joint replacements, bone plates, cardiovascular and spinal devices and in dental applications. There are reports regarding implant failures associate with increased local metal ion concentrations and macrophage populations. Macrophage cells are known to release NO and other reactive compounds (H_2O_2, O_2^-) and lower the local pH during inflammation and wound healing responses. The release of reactive oxidants (H_2O_2, O_2^-) may react with surface atoms and change the thickness and/or composition of the metal surface oxide and subsequently corrosion properties of the alloys. Macrophages lower the pH around implant site and create an acidic environment, which is known to accelerate the metal ion release process. Increased metal ion concentrations may lead to more inflammation and thus more metal ion release. This loop would eventually lead to implant failure. The roles of cells on alloy corrosion are not well understood and studied. Hence it was hypothesized in this study that 1. the behaviors of macrophage cells alter the alloys' corrosion behavior by changing its surface oxide and 2. the released metal ions from the alloys change the cell behavior.

To investigate these hypotheses, a series of *in vitro* experiments were designed to evaluate changes in surface composition and the corrosion behavior of alloys by macrophage cells under simulated clinical conditions. Macrophage cells were used because they were often found during inflammatory and would healing processes. The cellular responses to alloys and their released metal ions were evaluated based on viability, morphology and intracellular ATP (metabolic state) as well as effects on the release of inflammatory mediators NO and IL-1β.

Surface and Corrosion Properties

Both Co-Cr-Mo and Ti-6Al-4V alloys rely on a protective surface oxide layer for their corrosion resistance (ASTM F86). For use in clinical applications, the alloys are passivated using nitric acid (HNO_3) to increase the surface oxide thickness and corrosion resistance. Typically a Cr_2O_3/CrO_2 rich surface oxide with a small amount of Co oxide is formed on Co-Cr-Mo alloy and a predominantly TiO_2 oxide is formed on Ti-6Al-4V alloys (Strandman and Landt 1982; Kilpadi 1998; Milosev *et al*. 2000; Lee *et al*. 2000). The Co-Cr-Mo and Ti-6Al-4V alloy samples in this study also exhibited rich Cr_2O_3/CrO_2 and TiO_2 surface oxides respectively. Furthermore, analyses of the residual spectra did not reveal any differences in surface peaks for samples of each alloy in the as-polished and passivated state. Hence the surfaces of the alloys were consistent and typical of implant devices.

Milosev *et al*. (2000) reported a TiO_2 oxide is formed on the natural, air-exposed surface of the Ti-6Al-4V alloys. They noted that Al and V were not readily observed on

the surfaces until after sputtering. Lee *et al*. (2000) did observe Al but not V peaks on the cleaned and acid passivated Ti alloy surfaces. The result of this study demonstrated that the as polished and passivated Ti-6Al-4V surface was composed primarily of TiO_2 with a small amount of V_2O_3. No Al was observed on the surface. The differences between seeing Al and/or V peaks could be due to the different surface preparation (acid passivation vs. electrochemical passivation, with/without heat treatments) and the operating conditions of the machine (Al vs. Mg electrode, different pass energies and X-ray wattage used etc.). Nitric acid passivation was reported to increase the thickness of the Cr oxide in the surface and may introduce nitrogen species to the surface composition (Strandman and Landt 1982). Not many reports regarding surface examination on the Co-Cr-Mo were done in the past.

For both alloys the intensity of O and the major metal components that make up the metal oxides (Ti for Ti-6Al-4V and Cr for Co-Cr-Mo) increased with non-activated cells and activated cells compared to the surfaces exposed to medium. Ti and V peaks disappeared after incubating with medium for three days. The protein from the culture medium deposited on the surface most likely covered the alloy surface and masked the metal peaks because there was an increase in both carbon and nitrogen peaks after incubating with medium compared to as polished surfaces. After incubating with cells, especially activated cells, the Ti and O metal peaks increased in intensity. Cell metabolic activity may have increased the amount of oxide on the surface (Sundgren *et al.*, 1985) or cell attachment might have eliminated the amount of protein on the surfaces. Reactive chemical compounds such as H_2O_2 and O_2^- along with $NO^\cdot$ from activated cells may have

further enhanced the metal oxides on the surfaces as indicated from the high resolution (HR) spectra. The increase in metal oxide resulted in a more thermodynamically stable surface that reduced corrosion and metal ion release of the alloys in this study.

As for Co-Cr-Mo, the results were more variable. Activated cells seemed to induce more metal oxides on the surfaces compared to the other two conditions. But sometimes there was no difference in O and Cr peaks between all three conditions. Major peak of Co was often buried by the noise at the high binding energy end and Mo was not seen, which may due to its low concentration (~6%).

Examination of Ti implants extracted from patients after 6-8 years showed a marked increase in thickness of the surface oxide layer (Sundgren *et al*., 1986). Arys *et al*. (1998) proposed that oxide grows toward the bulk through metal and oxygen diffusion through the pores of the oxide. This might be due to a slow *in vivo* and *in vitro* oxidation process such as the reaction with released H_2O_2, O_2^- and $OONO^-$ (peroxynitrite). TiO_2 was reported to form a stable complex with H_2O_2 and $OONO^-$ released by macrophages (Suzuki and Frangos 2000; Ischiropoulos *et al*., 1992) and to have an anti-inflammatory characteristic (Overgaard *et al.*, 1998). The reactive nature of Ti oxide could be the reason its atomic percentage increase more than Cr oxide did with the released oxidants from activated macrophages.

Pan *et al*. (1998) reported that Ti pre-treated with H_2O_2 (100 mM for 30 days) had a 10-fold increase in thickness (60 nm) compared to the abraded surface (5-7 nm). The NO, H_2O_2, O_2^- released from the macrophage cells in this study may act on the surface similarly and affected the oxide thickness. They (Pan *et al*., 1996) also suggested that the

oxide film could be described by a two-layer model with a barrier inner layer and a porous outer layer. H_2O_2 addition results in an increased dissolution/oxidation rate that leads to an enhanced oxide growth of the porous outer layer. As a result, the total oxide film can reach a thickness corresponding to an interference blue color. Based on XPS results, H_2O_2 addition seems to further facilitate the incorporation of phosphate ions into the thicker porous layer. This observation may be related to the so-called osseointegration properties of titanium.

The enhancement of Ti oxides with activated cells was significant from both the atomic percentage analysis on the O and Ti percentages from the survey spectra and the O1s high-resolution spectra peak fit. As for Co-Cr-Mo, only the atomic percentage of O and Cr from survey spectra significantly increased with activated cells but the metal oxide peak did not show up in some of the O1s high-resolution peak fitting. One possible explanation for the difference between the two alloys is that Ti makes up 90 percentage in the bulk concentration and Cr only makes up ~28 percent. Although the percentage of Ti and Cr might both increase on the surface, still the changes in Ti oxide should be easier to measure with less percentage error for it was in a higher amount compared to Cr oxide. Also Ti has a higher affinity to oxygen than Cr (Clark and Williams, 1982) and might have responded more the oxidants.

The Cr peak showed up at the binding energy (BE) of ~576.6 eV, which was Cr in the state of Cr (III) (Cr_2O_3) and Cr (IV) (CrO_2). It was difficult to tell whether it was Cr_2O_3 or CrO_2 or both on the surface because Cr (III) and Cr (IV) have almost the same binding energy. The Ti2p peak showed up at ~ 458.6 eV and corresponded to the BE for

TiO_2. Kilpadi *et al*. (1998) also reported that Ti2p peak of TiO_2 was located around 458.5 eV. Peak fitting of the O1s peak on the Ti-6Al-4V in this study indicated that surface oxygen was present in three chemical states: the subpeak at 530-530.7 eV confirmed oxygen bound to Ti as TiO_2; subpeaks from 531-533 eV indicated intermediate Ti oxide species ($TiO_{1.0 \sim 1.65}$) as well as oxygen bound in organic forms and chemisorbed H_2O. Ti2p of TiO and Ti_2O_3 was at 455.4-455.8 eV and 457.2-457.6 eV respectively (Milosev *et al*., 2000) and were not seen on the Ti-6Al-4V surfaces in this study.

Nitrogen peak (N1s) was not found on as polished surfaces, indicating nitric acid passivation did not incorporate nitrate into the surface oxides of the alloys. The peak was observed with medium and cells present. N1s peak of all conditions could be fitted with a single peak at BE~401 eV, indicating the nitrogen species present on the surface in this study was most likely the N-H, C-N types of compounds, which could be the absorption of proteins from medium. No signs of nitrite (~404-405 eV), nitrate (~407 eV) and metal nitrides (~396.5-397.4 eV) were found on any surface, means NO from activated cells was not incorporated into the metal oxide even with oxidation process occurring.

The OCP data largely correlated to the changes in surface oxide observed from medium and cells releasing reactive chemicals. The OCP stayed the same over three days for Co-Cr-Mo for all conditions, indicating that the surface oxide of Co-Cr-Mo did not seem to change with time and test conditions. For Ti-6Al-4V for all conditions, OCP became more electropositive over three days, meaning the enhancement of the alloy surface oxide over time. The differences between the two alloys could be that Ti, which is the main constituent of the Ti alloy surface oxide, is a more reactive element than Cr,

which is the main constituent of the Co alloy surface oxide. It is more likely to react or incorporate with other elements present in the environment (Tengvall 1989; Esposito 1998; Suzuki 2000; Howlett 1999) and change on the surface more than Cr does.

Also, the OCP results corresponded to what we observed in metal oxide atomic percentage from the surface analysis. The surface with medium showed least amount of oxide, and it was noticed that when both alloys incubated with medium, OCP was most electronegative (reactive surface) compared to the rest of two conditions. The high electronegative behavior with medium was reflected in its total charge transfer; metal plates covered with plain medium generated highest total charge transfer compared to experiments with non-activated cells and activated cells. The lack of cells in plain medium environment might account for the low OCP (high surface reactivity) because cells attaching to the surface might prevent proteins from removing metal ions at the surface. Protein was reported to accelerate corrosion process by binding with the released ions (Ti, Cr) (Hallab *et al*., 2000). The cell culture medium used in this study contained 10% fetal bovine serum (3.5 wt % protein) and the effect of protein could be significant. The surface area exposed to protein in medium was higher compared to that with cells. At the double layer, ion concentrations were high and the bonding process of protein and ion changes the equilibrium and accelerated the dissolution process. Clark and Williams (1982) reported that the protein, serum albumin, increased the dissolution of Co, Cr, Ni, Cu. The bound protein underwent structural deformation and left the surface, replaced with another unbounded protein and the process repeats. Merrit and Brown (1988) reported that several proteins studied (albumin, globulin, transferrin and fibrinogen)

caused more weight loss and ion release from stainless steel plates and screws during fretting corrosion. Presence of albumin selectively leached Ni out of stainless steel alloys.

Both alloys, when incubated with cells became significantly more electropositive (less active surface) and, for Co-Cr-Mo, lower total charge transfers were measured as compared to the medium. The cell attachment, in addition to limiting the protein deposition, may limit oxygen diffusion to the surface. Less oxygen would lead to less oxidation-reduction reactions and thus less metal ion release and current flow. Also cells might act as a physical barrier for the ions to leave the surface (dissolution) or be removed by protein from the surface into solution. All these factors would result in less corrosion and metal ion release.

The total charge transfer and total metal ion release from both alloys showed that when cultured with activated cells, they generated significantly less amount of corrosion current and metal ions compared to the other two conditions (medium and cells). Though the OCP study did not show any difference between non-activated cells and activated cells, OCP was only an indication of the 'likelihood' of a reaction. It might not reflect the real situation in the short study. The current and metal ion reduction with activated cells might be attributed to the enhancement of metal oxide by the released reactive species rather than the physical presence of cell mono-layer since activated cells did not proliferate and attach to the surface much.

Metal ions

In this study, Co release was about four times higher that of Cr from Co-Cr-Mo after three days. Dorr *et al*. (1990) observed less Co (2 ppm) than Cr (12.5 ppm) in retrieved local tissue adjacent to Co-Cr-Mo hip implants, which was opposite from what we found. Hennig *et al*. (1992) also observed less Co (0.9 ppm) than Cr (3.5 ppm) in the tissue surrounding loose Co-Cr-Mo femeral shaft. The different environment (articulating *in vivo* system vs. non-articulating *in vitro* system), length of test, and surgical techniques (metal-on-metal or metal-on-plastic) could cause the difference in the amount of metal ion released (Sunderman *et al.* 1989).

With Ti-6Al-4V alloy, Ti concentration was similar to V when incubated with medium but 2-4 times higher than V when with non-activated cells and activated cells after three days. Considering Ti makes up 90% bulk concentration and V makes up only 4%, V was a more corrosive element compare to Ti. Dorr *et al*. (1990) saw more Ti in the fibrous tissue surroundig the Ti-6Al-4V hip implant than V (21 ppm Ti and 1 ppm V), also Lee *et al*. (2000) observed more Ti released into Hanks solution than V (50 ppb/cm^2 Ti and 2 ppb/cm^2 V) after one day, which was similar to our study with non-activated cells and activated cells.

With medium and cells, the released Co and Ti ion concentrations decreased over three days. Other ions seemed to decrease over time but not significantly. With activated cells, the amount of ion released did not seem to vary with time and was the lowest compared to with medium and cells. The decrease in metal ion release was thought to be due to the enhanced surface oxides by the release of reactive chemical species (oxidants)

from activated cells. Enhancement of the surface oxide over three days would lead to decreased corrosion as indicated by decreased total charge transfer and metal ion release. With activated cells, the amount of V release was reduced to 1/7 of that in medium and Co was 1/2 of that from medium. The significant decrease in the V and Co ion concentration with activated cells was attributed largely to the enhanced Ti and Cr surface oxides. The result of activated cells causing least metal ion release was consistent with their lowest total charge transfer. The ion release decreased over time was also found by other studies; Lee *et al*. (2000) found both Ti and V release decrease over time from acid passivated Ti alloy immersed in Hank's-EDTA solution for all different treatments (nitric acid passivated, 400^{o}C heat treated in air and aged in 100 ^{o}C water) over 16 days. The concentrations of Ti and V released on day 1 (~50 and 2 ppb/cm^2 respectively) in their study was higher than the concentration in this study (~0.5 and 1 ppb/cm^2 respectively). This may be due to different sterilization techniques and solutions used. Rae (1975) reported that Co-Cr-Mo particulate in cell culture medium released Co ion up to 3.4 ppm after one day and dropped to 1.7 ppm on day 2. The higher Co concentration compared to this study was mostly due to the use of metal particles instead of metal plates, which have lower surface area than particles. The Cr and Mo concentrations were below the detection limit (100 and 500 ppb) of the equipment used. Haynes *et al*. (2000) showed that artificially aged Co-Cr-Mo and 316L stainless steel particles (treated with acid) had less toxic effect on macrophages that ingested them as compared to the freshly produced particles. They reported particles with fresh surfaces released fewer metal ions over time as the oxide developed.

Mu *et al*. (2000) showed that rat peritoneal macrophage cells activated by polyethylene particles released 10 times more H_2O_2 compared to non-activated cells. The H_2O_2 caused pure Ti disks to release more Ti^{4+} ions (45 ppb) over a 28-day test period than those without H_2O_2 (30 ppb). The report only showed data from day 7 to day 28 with no indications on the detail from day 1 to day 3. H_2O_2 is also release by the macrophages in present study, which implies that if the tests were run longer than three days, H_2O_2 might result in disrrupted surface oxide and increased metal ion release.

Activated Macrophage Cells and Their Effects

The activated macrophage cells caused many differences compared to the two other conditions because they released nitric oxide (NO), hydrogen peroxide (H_2O_2) and superoxide ($O_2^{\cdot}$) among other inflammatory factors. All these reactive species were thought to either further oxidize the surface (increase metal oxides and corrosion resistance) or disrupt the existing metal oxides and increase corrosion. The result of this study suggested that they further oxidized the surface in three days. Possible mechanisms could be that hydrogen peroxide, in ambient conditions, will reduce to water and oxygen ($H_2O_2 \rightarrow H_2O + ½\ O_2$). The oxygen released might diffuse into the pores of the oxide and further react with the metal. Hydrogen peroxide also participates in the formation of hydroxyl radicals ($OH^{\cdot}$) in the presence of metal or metal ions ($M / M^{n+} + H_2O_2 \rightarrow M^{+}/M^{(n+1)+} + OH^{-} + OH^{\cdot}$) (Tengvall *et al*., 1989). Metal oxide on the surface (especially transition metals such as Ti, Cr and V) could thus be further oxidized by hydrogen peroxide. Superoxide rapidly reacts with nitric oxide to form peroxynitrite ($O_2. + NO \rightarrow$

O=N-O-O.) or nitrate (O_2. + NO $\rightarrow NO_3^-$). Peroxynitrite is a very reactive species which initiates oxidations and nitrations (Koppenol, 1998); nitrate (NO_3^-) may further passivate the metal surface ($M + NO_3^- \rightarrow M{=}O + NO_2^-$), which is why nitric acid is recommended for implant surface passivation in ASTM F86. Superoxide can also decompose into hydrogen peroxide when catalyzed by superoxidase dismutase (SOD) ($O_2^- + O_2^- + 2H^+ \rightarrow H_2O_2 + O_2$) and further oxidize metal and metal oxide as mentioned above. All these possible reactions could further increase metal oxide and possibly the oxide thickness; several *in vivo* and *in vitro* studies did demonstrate increases in oxide thickness after explantation (Arys 1998; Pan 1997; Sundgren 1985). Also, the possible mechanisms of reactive species reacting with metal surfaces would not cause any nitration of the surface metals, which is consistent with the findings from XPS surface analyses.

The data from surface analysis by X-ray Photoelectron Spectroscopy (XPS) showed that the surface with activated macrophages present had a significant amount of metal oxide enhancement and helped to improve corrosion resistance in a short period of time compared to the other two conditions. The enhancement of surface oxide was attributed to the reactive species released by activated macrophages. Similarly Pan *et al*. (1998) found H_2O_2 treated surfaces, after culturing with osteoblast-like cells, had increased corrosion resistance. They suggested that it might be the cell deposit that sealed the pore of the porous outer surface oxide layer and provided more corrosion resistance. Other types of cells, including macrophages, may deposit extracellular matrix and mask the pores and have similar effect to improve corrosion resistance.

Cellular Responses

The number of non-activated cells increased after three days on glass controls and the alloys. The numbers of cells were higher on the test alloys as compared to that to the controls. Warner *et al*. (1988) reported that in the presence of IFN-γ, Pb, Ni and Zn ions at less than 82, 28, 30 ppb respectively were able to induce proliferation of mice spleen lymphocytes. Though different metal ions were present in this study, low concentrations of metal ions (5-20 ppb) might have the similar effect on cell proliferation. Wang *et al.* (1996) reported Ti and Cr ions at 10 and 100 ppb significantly increased the proliferation of blood monocytes / macrophages, whereas Co did not. Ryhanen *et al*. (1997) reported the proliferation of human osteoblasts (OB) and fibroblasts (FB) increased on several metal implant materials; nitinol, Ti and stainless steel. The proliferation of FB was 108% (Nitinol), 134% (Ti) ($p < 0.02$) and 107% (Stainless steel) compared to the control cultures. The proliferation of OB was 101% (Nitinol), 100% (Ti) and 105% (Stainless steel) compared to the controls. Grimsdottir *et al.* (1994) found that nickel leached from metallic orthodontic appliances stimulated proliferation of lymphocytes from some of the nickel-sensitive subjects. Bearden and Cooke (1980) reported Co (7.5-30 ppm) inhibited the fibroblast proliferation, but the Co concentration in our study was much lower (<0.1 ppm) and might not have a significant effect on cell growth. Wataha *et al*. (1993) discovered that cell density might have effects on how fibroblast cells react to metal ions; at high density ($8x10^4$ /cm^2), the sensitivity of fibroblast toward metal ion toxicity (including Co^{2+}, Ti^{4+} and V^{3+}) decreased. The cell seeding density in our study was $1x10^5$ /cm^2 and thus they may not be responding much to the low dose of metal ions.

Hallab *et al*. (2001) reported that Cr from Co-Cr-Mo alloy degradation demonstrated approximately 10-fold greater reactivity to activated lymphocytes than Ti. The effects of the alloys' degradation products were greatest when the metals were complexed with high molecular weight proteins (approximately 180 kDa). Metal ions associated with protein, at low concentrations, could have positive effect on cell proliferation and viable macrophages could proliferate on a foreign surface as an immune response to the metal-protein complex.

The number of activated cells (cultured with LPS+IFN-γ) did not seem to increase after three days, either on the control or on the alloys. They seemed to decrease after three days compared to the seeding density. The activated cells produced reactive species, which were toxic to cells. Cells may detach from the surface due to toxicity from reactive species and were later removed from the sampling process. Cell debris was often found at the bottom of the sample tubes. The majority of activated cells remained on the surfaces were alive and contained similar ATP concentrations (metabolic activity) compared to the non-activated ones and those on the controls.

The majority of the non-activated cells and activated cells attaching to the surfaces of both alloys and the glass petri dish were shown to be viable. It was also noticed that non-activated cells had higher cell density on the surface than activated cells, both on the controls and the alloys. Wang *et al*. (1996) demonstrated that blood monocytes / macrophage cells exposed to Co, Cr and Mo from 0.01-100 ppb did not reduce cell viability by trypan blue exclusion and did not introduce cell injuries and cause cells to release lactate dehydorgenase (LDH). Although metal ion release was observed in

this study with the presence of non-activated cells and activated cells, the amounts of metal ions were at least 100 times lower than the 50% cytotoxicity concentration (ion concentration at which 50% of the extent of toxicity was observed) defined by Puleo and Huh, (1995), (Ti^{4+}=4ppm, Al^{3+}>25ppm, V^{5+}=2ppm, Co^{2+}=10ppm, Cr^{6+}=0.6ppm, Mo^{6+}>25ppm) and therefore were not expected to be toxic.

Haynes *et al*. (2000) concluded that passivated Co-Cr-Mo and 316L stainless steel particles released and exhibited lower toxic effects when ingested by macrophage cells as compared to fresh particles. This was because they saw these macrophages were able to release more pro-inflammatory cytokines (IL-6 and PGE_2). The macrophage cells in this study, exposed to low concentrations of metal ions, were able to release IL-1β and NO at concentrations similar to controls, indicating low concentrations of metal ions were not toxic to the cells and cells were as viable and functional as the controls.

Nichols and Puleo (1997) reported sublethal concentrations of metal ion release (Cr, Mo, Ti and V) did not affect osteoclast proliferation (protein content) but inhibited its osteolytic activity; the osteoclasts caused less resorption area on the bones with increased metal ion concentration. Thus they proposed, instead of inhibiting osteoclast activity, metal ions inhibited osteoblasts and thus the ability of bone to regrow and repair.

The SEM images showed that after three days, non-activated cells seemed to cover the metal surface more than the activated cells. This was consistent with the result from the cell count and Live/Dead tests that the non-activated cells proliferated more than the activated cells over the course of the test. The activated cells did not attach to the surface very well and the process of preparing the cells for SEM observation involved

many steps of changing solutions and rinsing. Even with extreme care, part of the cell population was probably removed from the surface. Thus SEM was not a good way to quantify cell numbers.

Qualitatively speaking, non-activated cells had more globular shape and smoother surface. They seemed to have more surface projections (membrane processes) attaching onto the metal and glass surfaces compared to the activated cells. Walkers *et al*. (1974) had similar findings. Activated cells seemed larger (Loike *et al*., 1979), more elongated and with more surface extensions but less membrane processes attaching to the substrates compared to the non-activated ones. Again, this was also similar to the result found by the Waters *et al*., 1975. They used rabbit alveolar macrophages incubated with 5 ppm V ion for 20 hours, and they found the activated macrophages had less membrane attachment, and viability was reduced by 10%. The metal ions in this study were much lower than 5 ppm (max ~ 50 ppb) and thus was not believed to be toxic to the non-activated cells, but morphological change after stimulation could be similar.

The Live/Dead test showed high viability of non-activated cells and activated cells on both glass controls and test alloys and at the same time the cells exhibited the morphology that was seen from previous studies. Cells had same viability and regular morphology on both controls and metals was attributed to the low doses of metal ions detected in the supernatant, way lower than 50% toxicity concentrations. These alloy plates are not stimulatory to the macrophage cells and are known in general to be well tolerated by tissues, thus their wide spread use in the implant industry.

The intracellular ATP concentrations were not different between controls and metal alloys, neither between non-activated cells and activated cells. Concentrations of ATP were similar to that of non-activated macrophages reported by Loike *et al*. (1979), which was around $5x10^{-16}$ moles per cell. They reported intracellular ATP in resident macrophage was near $5x10^{-16}$ mole/cell and $12x10^{-16}$ mole/cell in activated cells. This again demonstrated the non-toxic and biocompatible natures of the alloys.

Previous studies regarding intracellular ATP concentrations in activated lymphocytes varied. Crouch *et al.* (1993) reported LPS+IFN-γ activated cells had more intracellular ATP than non-activated cells. On the other hand, Bradbury *et al*. (2000) and Moss *et al*. (2001) have shown the opposite; more viable and proliferating cells had higher intracellular ATP concentrations compared to the LPS+IFN-γ activated cells and cells undergoing apoptosis. Armstrong *et al*., (1991) did a study on the hamster ovary cells under chemical treatments and concluded that ATP in treated cells varied over time and was dose dependent. Changes were likely due to the metabolic perturbations or altered cell biomass. Depending on the design of the experiment and time of measurement, ATP concentrations are hard to compare between laboratories. Loike *et al*. (1979) also reported that ATP concentration was not a good indication of cell activation (phagocytosing mouse peritoneal macrophages) because their study found ATP in macrophage cells during ingestion had not changed, but its specific activity was 40% lower than controls. The phagocytosing cells, instead of using ATP as energy source, used creatine phosphate as an alternate energy source. Oosting *et al*. 1991 demonstrated that mouse alveolar macrophage showed ATP depletion when exposed to H_2O_2 but when

exposed to ozone (O_3 in PBS solution), ATP increased. This indicated ATP concentrations did not exactly correlate to macrophage activation. ATP might have increased at some point of time but was later depleted by the presence of H_2O_2. Depletion of cellular energy stores by oxidants generated during inflammation *in vivo* may be a means by which the inflammatory response is self-limited (Sporn and Peters-Golden, 1988). In this study, H_2O_2 might have depleted ATP in activated cells such that no ATP increase was observed compared to non-activated cells at the end of the tests, or, it was because macrophages were using the alternate energy source rather than ATP. For a complicated system factors like different surfaces, the released metal ions or even the imposed voltage could have effects on ATP concentrations as well.

Nitric oxide is synthesized by NO synthase (NOS) inside cells and diffused freely across the membrane. It is quickly consumed around cells that secrete it due to its highly unstable nature and acts as a paracrine or autocrine. It has been known to be one of the neurotransmitters of some motor neurons of the parasympathetic nervous system; it can mediate inflammation and act on endothelial cells to cause increased local blood flow (Bevilacqua, 1993) to facilitate the delivery of leukocytes. More recently, NO produced by the osteoblasts has been proposed to promote bone resorption by osteoclasts (van't Hof and Ralston, 1997; Riancho *et al.*, 1995). Only the activated cells released NO. NO was detectable at day 1 and increased over time. The activated cells were not suppressed or further activated by the test alloys or the released metal ions when compared to the controls. Besides the low concentrations of released metal ions, activated cells did not attach well and that might be why they did not respond to different surfaces (metals or

glass). The non-activated macrophage cells did not release NO at all and were not activated by the metal surfaces and low dose of metal ions. Metal ion concentrations could increase over time (Mu 2000) by accumulating locally. Higher concentrations of metal ions may eventually activate macrophage cells to release NO (Wataha *et al.* 1995 and 1996).

Though NO release by macropahge cells does not directly cause oxidization and changes of surface oxide, it was measured in this study for the sole purpose of ensuring cell activation over three days. Hydrogen peroxide and superoxide are known to be released by this cell line (Raw 264.7) as long as cells were activated. Unlike O_2^- and H_2O_2 which concentrations were reported to be low and decrease to almost zero within 5-10 hrs, amount of NO release was higher and its product NO_2^- remains stable in solution and could be measured over three days. Pfeiffer *et al.* (2001) reported LPS+IFN-γ activated macrophage (Raw 264.7 cell line) released maximum amount of 125 pmole/min/mg cell of NO within one day, compared to 15 pmole/min/mg cell of O_2^- and 2 pmole/min/mg cell of H_2O_2. In this study, significant enhancement of metal surface oxide was observed in the period of three days with the release of nitric oxide, hydrogen peroxide and superoxide; though the exact mechanisms remain unknown. The changes of the surfaces resulted in a decrease in the amount of metal ion release and the decrease in corrosion over three days.

IL-1β is a major mediator of the host inflammatory response in innate immunity. It acts on fibroblasts to regulate their proliferation and induces vascular endothelial cells to express surface receptors that render these cells more adhesive to leukocytes. The

amount of IL-1β released by non-activated cells remained low (<10 pg/ml) and did not increase over time. With activated cells, the IL-1β concentration in the supernatant increased over three days. The release of IL-1β from activated cells was generally low the first day, almost the same as non-activated cells. But in day 2 and day 3, the amount of IL-1β increased significantly compared to day 1. Interestingly, activated cells seemed to release more IL-1β on the metal surface compared to the control (glass surface). This could be due to the low concentrations of metal ions according to Wang *et al*., 1996. They demonstrated that non-activated blood macrophage cells did not release more IL-1β in the presence of metal ions (Ti, Co and Cr from 0.01-100 ppb) compared to the controls (no metal ions). However, activated macrophages secreted 1.2 and 1.3 times more IL-1β in the presence of metal ions (100 ppb Ti and 100 ppb Cr, respectively) than macrophages from the control cells. This is consistent with our finding that activated cells release more IL-1β when cultured on alloys compared to those on the glass.

In general, non-activated macrophage cells growing on the alloys' surfaces showed similar viability, morphology, metabolic state (intracellular ATP concentration) and higher proliferation when compared to controls. The results seem to indicate that the tested alloys were compatible with non-activated macrophage cells. As a matter of fact, these alloys have long been used for implant applications and are considered very biocompatible.

In three days, non-activated macrophages growing on alloys did not show any sign of activation (NO increase) with the low dose of released metal ions and were well

adapted to the alloys' surfaces (good viability). Release NO and the IL-1β concentrations were low and similar to that from the controls.

For LPS + IFN-γ activated macrophages growing on alloys, the cells had decreased proliferation and different morphology than the non-activated cells. Even so, they remained viable on the surface and their intracellular ATP concentrations were similar to those of non-activated cells, which were similar to the findings of Loike *et al*., 1979.

On average, activated cells released more IL-1β per cell on the alloy surfaces than the control on day 3. One possible reason is that the metal surfaces and release metal ions might have a synergistic effect with LPS + IFN-γ on the release of pro-inflammatory cytokines. But the activated cells did not seem to release more NO/cell on the alloys than the controls, meaning the metal surface and low dose of released metal ions did not affect NO release from activate the cells. With further enhance metal oxides and reduced corrosion with activated cells, alloys were not expected to release more metal ions and affect the activated macrophage cells compared to with non-activated cells.

CHAPTER V
CONCLUSIONS AND FUTURE WORK

The hypothesis that macrophage cells and their released inflammatory compounds have effects on the two alloys was supported by the results of this study. The results demonstrated that cells had significant effects on surface composition, ion release and thus corrosion properties of Co-Cr-Mo and Ti-6Al-4V implant alloys. Especially with activated cells, which release reactive oxygen and nitrogen species, the effects were even more profound. The release of reactive species by the cells enhanced alloy surface oxides, which reduced metal ion release and corrosion in three days.

The alloys and the low concentration of ion release did not seem to affect the growth, viability, morphology or intracellular ATP concentrations of non-activated macrophage cells. When cultured on alloys, the cells were not activated to release NO or significant amounts of IL-1β. These two metal alloys could be considered highly biocompatible with non-activated macrophage *in vitro*. Similarly, the alloys and low concentrations of released metal ions were well tolerated by the activated cells though increased IL-1β was measured with the alloys as compared to glass controls. Though in three days the alloys and their released metal ions did not significantly change the

functions of either non-activated or activated macrophages as it was hypothesized (the alloy corrosion products further activate the macrophage cells and induce more inflammatory reactions), longer studies are needed to further evaluate this issue.

Several things are worth trying to further investigate with regard to the interactions between the cells and the materials;

1. Longer testing periods. The three-day tests seem short and might not simulate real long-term metal behaviors properly.

2. Observation of surface oxide structure and thickness with SEM. Observation of the section perpendicular to the surface might give a better perspective about the structural change with different culture conditions.

3. Experiments with primary human macrophage cells. Transformed mouse tumor macrophage cells might not reflect the real behavior of human primary macrophage cells.

4. Evaluate corrosion behaviors at micro levels- pH, O_2 and released chemicals may vary greatly locally at cell-metal interface as compared to the bulk, and so is the corrosion behaviors.

BIBLIOGRAPHY

Al-Bayati MA, Giri SN, Raabe OG, Rosenblatt LS, Shifrine M. Time and dose-response study of the effects of vanadate on rats: morphological and biochemical changes in organs. *J Environ Pathol Toxicol Oncol* 1989 Dec;9(5-6):435-55.

Amstutz HC, Campbell P, Kossovsky N, Clarke IC. Mechanism and clinical significance of wear debris induced osteolysis. *Clin Orthop* 1992; 276:7-18.

Armstrong MJ, Bean CL, Galloway SM. A quantitative assessment of the cytotoxicity associated with chromosomal aberration detection in Chinese hamster ovary cells. *Mutat Res*. 1992, 265 (1): 45-60.

Arys A, Philippart C, Dourov N, He Y, Le QT, Pireaux JJ. Analysis of titanium dental implant after failure of osseointegration: combined histological, electro microscopy, and x-ray photoelectron spectroscopy approach. *J Biomed Mater Res* 1998; 43: 300-312.

Bearden L and Cooke F. Growth inhibition of cultured fibroblasts by cobalt and nickel. *J Biomed Mater Res*. 1980 May; 14(3): 289-309.

Bevilacqua MP. Endothelial-leukocyte adhesion molecules. *Ann Rev Immunol* 1993. 11: 767-804.

Bianco Ducheyne P, Cuckler JM. Local accumulation of titanium released from a titanium implant in the absence of wear. *J Biomed Mater Res* 1996, 31:221-234.

Black J, Oppenheimer P, Morris DM, Peduto AM, Clark CC. Release of corrosion products by F-75 cobalt base alloy in the rat. III: Effects of a carbon surface coating. *J Biomed Mater Res* 1987 Oct; 21(10):1213-30.

Black J. `Corrosion and degradation' ln Orthopedic biomaterials in research and practice, New York, Churchill, Livingstone, 1988: 235-266.

Black J. In vitro and in vivo corrosion of chromium passivated alloy and some biological consequences. *Proceeding of the symposium on compatibility of biomedical implants.* Eds. Kovacs P and Istephanous NS. Vol 94-15, 35-41.

Bouchard R *et al.,* Tumorgenicity of F-75 CoCrMo and F-136 Ti6Al4V in the at: relationship to implant-tissue motion. *Trans 4th World Cong Biomaterials* 1992, 280.

Boyd C and DeVault V. Physics. Austin, Tex., Steck-Vaughn Co. (1959).

Bradbury DA, Simmons TD, Slater KJ, Crouch SP. Measurement of the ADP:ATP ratio in human leukaemic cell lines can be used as an indicator of cell viability, necrosis and apoptosis. *J Immunol Methods*. 2000 23; 240(1-2): 79-92.

Brown S and Merritt K. Fretting corrosion in saline and serum. *J Biomed Mater Res* 1981, 15, p479-488.

Brown SA, Zhang K, Merritt K and Payer JH. *In vivo* transport and excretion of corrosion products from accelerated anodic corrosion of porous coated F75 alloy. *J Biomed Mater Res* 1993, 27, p1007-1017.

Bruneel N and Helson JA. *In vitro* simulation of biocompatibility of Ti-Al-V. *J Biomed Mater Res* 1988, 22, 203.

Bumgardner JD, Doeller J and Lucas LC. Effect of nickel-based dental casting alloys on fibroblast metabolism and ultrastructural organization. *J Biomed Mater Res*. 1995; 29(5): 611-7.

Bundy KJ. Characterization of the corrosion behavior of porous materials by AC impedance techniques, in quantitative characterization and performance of porous implants for hard tissue application, JE Lemons Ed., STP 953, ASTM, Philadelphia, 1987, 137.

Bundy KJ. Corrosion and other electrochemical aspects of biomaterial. *Crit Rev Biomed Eng* 1994, 22(3/4): 139-251.

Bundy KJ. Fundamental effects governing soft tissue adhesion to biomaterials. Trans. 4th World Biomaterials Congr., 1992, 348.

Callen BW, Lowenberg BF, Lugowski S, Sodhi RN, Davies JE. Nitric acid passivation of Ti6Al4V reduces thickness of surface oxide layer and increased trace element release. *J Biomed Mater Res*, 29, 279-290, 1995.

Callister WD. Materials science and engineering: An introduction. 5th Ed, John Wiley & Sons, Inc. 2000.

Chen F, Vallyathan V, Castranova V, Shi X. Cell apoptosis induced by carcinogenic metals. *Mol Cell Biochem*. 2001 Jun;222(1-2):183-8.

Chohayeb AA, Franker AC, Eichmiller RM, Waterstrat RM and Boyd J. Corrosion behavior of dental casting alloys coupled with titanium. Medical Application of Titanium and Its Alloys: The Material and Biological Issues, ASTM STP 1272, S Brown and J Lemons, Eds, American Society fir Testing Materials 1996.

Clark GCF and Williams DF. The effects of proteins on metallic corrosion, *J Biomed Mater Res 1982*, 16, p125-134.

Coleman RF, Herrington J, Scales JT. Concentrations of wear products in hair, blood and urine after total hip replacement. *Br Med J* 1973, 1, 527.

Cornelini R, Artese L, Rubini C, Fioroni M, Ferrero G, Santinelli A, Piattelli A. Vascular endothelial growth factor and microvessel density around healthy and failing dental implants. *Int J Oral Maxillofac Implants* 2001 May-Jun;16(3):389-93.

Crouch S, Kozlowski R, Slater KJ, Fletcher J. The use of ATP bioluminescence as a measure of cell proliferation and cytotoxicity. *J Immunol Methods* 1993 Mar 15; 160(1): 81-8.

das Neves RP, Santos TM, de Pereira ML, de Jesus JP. Cr (IV) induced alternations in mouse spleen cells: a short-term assay. *Cytobios* 2001; 106 suppl 1:27-34.

Diane M. Stearns, Kevin D. Courtney, Paloma H. Giangrande, Laura S. Phieffer, and Karen E. Wetterhahn**.** Chromium(VI) Reduction by Ascorbate: Role of Reactive Intermediates in DNA Damage *In Vitro*. Molecular Mechanisms of Metal Toxicity and Carcinogenicity Environmental Health Perspectives 102, Supplement 3, September 1994.

Dobbs HS and Minski MJ. Metal ion release after total hip replacement, in Biomaterials 1980. John Wiley, New York, 1982, 225.

Donati ME, Savarino L, Granchi D, Ciapetti G, Cervellati M, Rotini R, Pizzoferrato A. The effect of metal corrosion debris on immune system cells, *Chir Organi Mov* 1998, 83(4): 387-393.

Doran A, Law FC, Allen MJ, Rushton N. Neoplastic transformation of cells by soluble but not particulate forms of metals used in orthopedic implants. *Biomaterials* 1998; 19: 751-759.

Dorr LD, Bloebaum R, Emmanual J, Meldrum R. Histologic, biochemical, and ion analysis of tissue and fluids retrieved during total hip arthroplasty. *Clin Orthop*. 1990; 261:82-95.

Ducheyne P. Enhanced metal ion release from Ti and its alloys. Trans 12th Annu Meeting Soc Biomaterials 1986, p183.

Escalas F, Galante J, Rostoker W. Biocompatibilities of materials for joint replacement. *J Biomed Mater Res* 1976, 10:175-195.

Esposito M, Lausmaa J, Hirsch JM, Thomsen P. Surface analysis of failed oral titanium implants. *J Biomed Mater Res* 1999; 48: 559-568.

Evans EJ and Thomas IT. The in vitro toxicity of cobalt-chromium-molybdenum alloy and its constituent metals. *Biomaterials* 1986, 7:25-29.

Fontana MG. Corrosion engineering. New York: McGraw-Hill, c1986.

Georgette FS. Effect of hot isostatic pressing on the mechanical and corrosion properties of cast, porous-coated Co-Cr-Mo alloy; in Quantitative characterization and performance of porous implant for hard tissu application, ASTM STP 953. J Lemons (ed), ASTM 1987, 31-46.

Gerhardsson L, Bjorkner B, Karlsteen M, Schutz A. Copper allergy from dental copper amalgam? *Sci Total Environ* 2002 May 6;290(1-3):41-6.

Gilbert TL, Buckley CA, Jacobs JJ. In vivo corrosion of modular hip prosthesis components in mixed and similar combinations. The effect of crevice, stress, motion and stress coupling. *J Biomed Mater Res* 1993, 27: 1533 – 1544.

GoldringSR, Schiller AL, Roelke M, Rourke CM, O'Neil DA, Harris WH. The synovial-like membrane at bone-cement interface in loose total hip replacements, and its proposed role in bone lysis. *J Bone Joint Surg Am* 1983; 65(A): 575-584.

Goldring SR, Jasty M, Roelke MS, Rourke CM, Bringhurst FR, Harris WH. Formation of a synovial-like membrane at bone-cement interface: its role in bone resorption and implant loosening after total hip replacements. *Arth Rheum* 1986; 29: 836-842.

Granchi D; Verri E; Ciapetti G; Savarino L; Cenni E; Gori A; Pizzoferrato A. Effects of chromium extract on cytokine release by mononuclear cells. *Biomaterials* 1998 Jan-Feb; 19 (1-3), pp. 283-91.

Granchi D *et al.,* Cell death induced by metal ions: necrosis or apoptosis? *J Mater Sci, Mater Medicine* 1998; 9: 31-37.

Granchi D, Ciapetti G, Stea S, Savarino L, Filippini F, Sudanese A, Zinghi G, Montanaro L. Cytokine release in mononuclear cells of patients with Co-Cr hip prosthesis. *Biomaterials* 1999; 20(12): 1079-1086.

Granchi D, Ciapetti G, Savarino L, Stea S, Filippini F, Sudanese A, Rotini R, Giunti A. Expression of the CD69 activation antigen on lymphocytes of patients with hip prosthesis. *Biomaterials*. 2000; 21(20): 2059-65.

Griffin CD, Buchanan RA, Lemons JE. In vivo electrochemical corrosion study of coupled surgical implant materials. *J Biomed Mater Res* 1983; 17: 489 – 500.

Grimsdottir MR, Hensten-Pettersen A, Kullmann A. Proliferation of nickel-sensitive human lymphocytes by corrosion products of orthodontic appliances. *Biomaterials* 1994 Nov;15(14):1157-60.

Hallab N, Vermes C, Messina C, Roebuck KA, Glant TT, Jacobs JJ. Concentration- and composition-dependent effects of metal ions on human MG-63 osteoblasts. *J Biomed Mater Res* 2002; 60: 420-433.

Hallab N, Mikecz K, Vermes C, Skipor A, Jacobs JJ. Differential lymphocyte reactivity to serum-derived metal-protein complexes produced from cobalt-based and titanium-based implant alloy degradation. *J Biomed Mater Res* 2001. 56(3):427-36.

Hallab N, Merritt K and Jacobs JJ. Metal sensitivity in patients with orthopaedic implants. *J Bone Joint Surg Am*. 2001; 83-A(3):428-36. Review.

Hallab N**,** Jacobs JJ, Skipor A, Black J, Mikecz K, Galante JO. Systemic metal-protein binding associated with total joint replacement arthroplasty. *J Biomed Mater Res* 2000. 49(3):353-61.

Haynes D, Crotti TN, Haywood MR. Corrosion of and changes in biological effects of Cobalt chrome alloys and 316L Stainless steel prosthetic particles with age. *J Biomed Mater Res* 2000, 49: 167-175.

Hennig FF, Raithel HJ, Schaller KH, Dohler JR. Nickel-, chrom- and cobalt-concentrations in human tissue and body fluids of hip prosthesis patients. *J Trace Elem Electrolytes Health Dis*. 1992; 6(4):239-43.

Howlett CR, Zreiqat H, Wu Y, McFall DW, McKenzie DR. Effect of ion modification of commonly used orthopedic materials on the attachment of human bone-derived cells. *J Biomed Mater Res* 1999; 45: 345-354.

Huang H. Effect of chemical composition on the corrosion behavior of Ni-Cr-Mo dental casting alloys. *J Biomed Mater Res* 2002; 60: 458-465.

Imam M and Fracker A., Titanium alloys as implant materials. Medical Application of Titanium and Its Alloys: The Material and Biological Issues, ASTM STP 1272, S Brown and J Lemons, Eds, American Society fir Testing Materials 1996.

Ingham E and Fisher J. Biological reactions to wear debris in total joint replacement. *Proc Inst Mech Eng* H 2000; 214(1): 21-37.

Irby M and Marek M., The Galvanic interaction between dissimilar orthopedic implant alloys.

Ischiropoulos H, Zhu L, Beckman JS. Peroxynitrite formation from macrophage-derived nitric oxide. *Arch Biochem Biophys* 1992; 198: p446-451.

Jacobs JJ, Latanision RM, Rose RM, Veeck SJ. The effect of porous coating processing on the corrosion behavior of Co-Cr-Mo surgical implant alloys. *J Orthop Res* 1990, 8: 874-882.

Jacobs JJ, Skipor AK, Patterson LM, Hallab NJ, Paprosky WG, Black J, Galante JO. Metal release and excretion from cememtless total knee replacement. *Clin Orthop* 1999; 358: 173-180.

Jobin M. Hydroxylation and crystallization of electropolished Ti surface. Ultramicroscopy, May/June 1992.

Kanerva L and Forstrom L. Allergic nickel and chromate hand dermatitis induced by orthopaedic metal implant. *Contact Dermatitis* 2001; 44(2): 103-4.

Kavanagh BF, Wallrichs S, Dewitz M, Berry D, Currier B, Ilstrup D, Coventry MB. Charnley low-friction arthroplasty of the hip: 20-year results with cement. *J Arthroplasty* 1994; 9:229-234.

Kawalec JS, Brown SA, Payer JH, Merritt K. Mixed metal fretting corrosion of Ti6Al4V and wrought Cobalt alloy. *J Biomed Mater Res* 1995, 29 (7): 867-873.

Kawanishi S, Hiraku Y, Murata M, Oikawa S. The role of metals in site-specific DNA damage with reference to carcinogenesis. *Free Radic Biol Med* 2002 May 1;32(9):822-32.

Kilpadi DV, Raikar GN, Liu J, Lemons JE, Vohra Y, Gregory JC. Effect of surface treatment on unalloyed Ti implants: Spectroscopic analysis, *J Biomed Mater Res*, 40, 646-659, 1998.

Kolman DG and Scully JR. Electrochemistry and passivity of Ti-15V-3Cr-3Al-3Sn beta-Ti alloy in ambient temperature aqureous chloride solutions. *J Electrochem Soc* 1994, 141 (10): 2633-2641.

Koppenol WH. The baisc chemistry of nitrogen monoxide and peroxynitrite. *Free Radic Biol Med* 1998, 25: 385-391.

Kovacs P. Electrochemical basics of fretting accelerated crevice corrosion. *Trans Soc Biomat* 1993, 19: 272.

Kovacs P. Ion release of implant metal bearing surfaces. *Trans 16th Annu Meeting Soc Biomaterials* 1990, p198.

Laffargue P, Hildebrand HF, Lecomte-Houcke M, Biehl V, Breme J, Decoulx J**.** Malignant fibrous histiocytoma of bone 20 years after femoral fracture treated by plate-screw fixation: analysis of corrosion products and their role in malignancy. *Rev Chir Orthop Reparatrice Appar Mot*. 2001 Feb 1;87(1):84-90.

Lee SH, Brennan FR, Jacobs JJ, Urban RM, Ragasa DR, Glant TT. Human monocyte/macrophage response to cobalt-chromium corrosion products and titanium particles in patients with total joint replacements. *J Orthop Res* 1997 Jan; 15(1): 40-9.

Lee TM, Chang E, Yang CY. A comparison of the surface characteristics and ion release of TiAlV and heat treated TiAlV. *J Biomed Mater Res* 2000. 50:499-511.

Leopold SS, Berger RA, Patterson L, Skipor AK, Urban RM, Jacobs JJ. Serum titanium level for diagnosis of a failed, metal backed patellar component. *J Arthroplasty* 2000; 15(7): 938-943.

Liu HC, Chang WH, Lin FH, Lu KH, Tsuang YH, Sun JS. Cytokine and prostaglandin E2 release from leukocytes in response to metal ions derived from different prosthetic materials: an in vitro study. *Artif Organs* 1999 Dec; 23(12): 1099-106.

Liu KJ and Shi X. In vivo reduction of chromium (VI) and its related free radical generation. *Mol Cell Biochem*. 2001 Jun;222(1-2):41-7.

Loike J, Kozler VF, Silverstein SC. Increased ATP and creatine phosphate turnover in phagocytosing mouse peritoneal macrophages. *J Biol Chem*. 1979 Oct 10; 254(19): 9558-64.

Lucas LC. Ultrastructural examination of in vitro and in vivo cells exposed to elements from type 316L stainless steel. Corrosion and degradation of implant materials: second symposium, ASTM STP 859. Editors: A Franker and C Griffin. ASTM, Philadelphia, 1985, pp 208-222.

Lundin A. Extraction and automatic luminometric assay of ATP, ADP and AMP, In: *Analytical applications of bioluminescence and chemiluminescence*. Academic Press: New York, 237-249, 1979.

Mak KH, Wong TK, Poddar NC. Wear debris from total hip arthroplasty presenting as an intrapelvic mass. *J Arthroplasty* 2001 Aug;16(5):674-6.

Mansfeld F. Application of electrochemical impedance spectroscopy to the evaluation of the corrosion behavior of implant materials. Proceedings of the symposium on compatibility of biomedical implants. The electrochemical society, Inc., NJ. P59-72.

Marek M., Measurement of metal ion release from biomedical implant alloys. Proceedings of the symposium on compatibility of biomedical implants. The electrochemical society, Inc., NJ. P73-84.

Mauesli PA. Constitution of oxides on Ti alloy for surgical implants, in Implant Materials in Biofunction. Elsevier, Amsterdam, 1988, 305.

Memoli VA, Urban RM, Alroy J, Galante JO. Malignant neoplasms associated with orthopedic implant materials in rats. *J Orthop Res* 1986; 4(3): 346-55.

[a] Messer RL, Bishop S and Lucas LC. Effect of metallic ion toxicity on human gingival fibroblasts morphology. *Biomaterials* 1999; 20(18): 1647-57.

[b] Messer RL and Lucas LC. Evaluations of metabolic activities as biocompatibility tools: a study of individual ion's effect on fibroblasts. *Dent Mater* 1999; 15 (1): 1-6.

Merritt, K. Allergic reactions to materials used in prosthetic surgery. *Biomaterials* 1987, 7:711-716.

Merritt K. Biochemistry/Hypersensitivity/Clinical Reaction. International workshop on biocompatibility, toxicity and hypersensitivity to alloy systems used in dentistry, Ann Arbor, 1986.

Merritt K and Brown S. Effect of proteins and pH on fretting corrosion and metal ion release. *J Biomed Mater Res* 1988. 22(2): 111-120.

Merritt K and Brown S. Effect of valence chromium on biological responses. *Biomaterials and biomechanics*, 1983.

Merritt, K, Crowe TD and Brown SA. Elimination of nickel, cobalt and chromium following repeated injections of high dose metal salts. *J Biomed Mater Res* 1989, 23:845.

Merritt, K. Role of medical materials both in implant and surface applications in immune response and resistance to infection. *Biomaterials* 1984, 5:47-53.

Miller K and Anderson J. Human monocyte/macrophage activation and interlukin-1 generation by biomedical polymers. *J Biomed Mater Res* 1988; 22:713-731.

Miller K, Rose-Caprara V, Anderson JM**.** Generation of IL-1 activity in response to biomedical polymer implants: A comparison of *in vitro* and *in vivo* models. *J Biomed Mater Res* 1989; 23: 1007-1026.

Milosev I, Metikos-Hukovic M, Strehblow HH. Passive film on orthopedic TiAlV alloy formed in physiological solution investigated by X-ray photoelectron spectroscopy. *Biomaterials*, 21, 2103-2113, 2000.

Misra M, Alcedo JA, Wetterhahn KE. Two pathways for chromium(VI)-induced DNA damage in 14 day chick embryos: Cr-DNA binding in liver and 8-oxo-2'-deoxyguanosine in red blood cells. *Carcinogenesis* 1994; 15(12): 2911-7.

Mora N, Cano E, Mora EM, Bastidas JM. Influence of pH and oxygen on copper corrosion in simulated uterine fluid. *Biomaterials* 2002 Feb;23(3):667-71.

Morais S, Carvalho GS, Faria JL, Gomes HT, Sousa JP. In vitro biomineralization by osteblast cells. I: retardation by tissue mineralization by metal salts. *Biomaterials* 1998; 19: 13-21.

Moss DW and Bates TE. Activation of murine microglial cell lines by lipopolysaccharide and interferon-gamma causes NO-mediated decreases in mitochondrial and cellular function. *Eur-J-Neurosci.* 2001 13(3): 529-38.

Mu Y, Kobayashi T, Sumita M, Yamamoto A, Hanawa T. Metal ion release from titanium with active oxygen species generated by rat macrophages *in vitro*. *J Biomed Mater Res* 2000. 49:238-243.

Mueller HJ. Electrochemical charge and protein adsorption. *Mater Res Symp* 1989, 110, 605.

Mustafa K, Pan J, Wroblewski J, Leygraf C, Arvidson K. Electrochemical impedance spectroscopy and X-ray photoelectron spectroscopy analysis of titanium surfaces cultured with osteoblast-like cells derived from human mandibular bone. *J Biomed Mater Res*. 2002 Mar 15;59(4):655-64.

Nasu T, Suzuki N. Effects of aluminum ions on K(+)-induced contraction in ileal longitudinal smooth muscle. *Comp Biochem Physiol C Pharmacol Toxicol Endocrinol* 1998 Jul;120(1):137-43.

Nichols KG and Puleo DA. Effect of metal ions on the formation and function of osteoclasts *in vitro*. *J Biomed Mater Res* 1997; 35(2): 265-271.

O'Brien B, Carroll WM, Kelly MJ. Passivation of nitinol wire for vascular implants--a demonstration of the benefits. *Biomaterials* 2002 Apr;23(8):1739-48.

Ohnsorge J and Holm R. Surface investigations of oxide layers on Co-Cr alloyed orthopedic implants using ESCA technique. *Med Prog Technol*, 5, 171-177, 1978.

Omanovic S, Roscoe SG. Interfacial Behavior of beta-Lactoglobulin at a Stainless Steel Surface: An Electrochemical Impedance Spectroscopy Study. *J Colloid Interface Sci* 2000 Jul 15;227(2):452-460.

Oppenheim WL, Namba R, Goodman WG, Salusky IB. Aluminum toxicity complicating renal osteodystrophy. *J Bone Joint Surg* 1989, 71A: 446-452.

Oosting RS, Van Rees-Verhoef M, Verhoef J, Van Golde LM, Van Bree L. Effects of ozone on cellular ATP levels in rat and mouse alveolar macrophages. *Toxicology* 1991, 70: 195-202.

Overgaard L, Danielsen N, Bjursten LM. Anti-inflammatory properties of titanium in the joint environment. *J Bone Joint Surg* 1998. 80B: p888-893.

Pan J, Liao H, Leygraf C, Thierry D, Li J. Variation of oxide films on Ti induced by osteoblast-like cell culture and the influence of an H_2O_2 pretreatment. *J Biomed Mater Res* 1998. 40(2), 244-256.

Pan J, Thierry D, Leygraf C. Electrochemical and XPS studies of titanium for biomaterial applications with respect to the effect of hydrogen peroxide. *J Biomed Mater Res* 1994. 28:113-122.

Pan J, Thierry D, Leygraf C. Hydrogen peroxide toward enhance oxide grow on titanium in PBS solution. *J Biomed Mater Res* 1996. 30:393-402.

Park JB and Lakes RS. Biomaterials: An introduction. Plenum Press, NY, NY. P79-114, 1992.

Park JB. Biomaterials Science and Engineering. Plenum Press. New York, 1984

Parker SH and Bumgardner JD. Master' Thesis. 2001. Biomedical Engineering Program, Mississippi State University.

Pfeiffer S, Lass A, Schmidt K, Mayer B. Protein tyrosine nitration in cytokine-activated murine macrophages. *J Biol Chem* 2001, 276(36): 34051-8.

Placko HE, Brown SA, Payer JH. Effects of microstructure on the corrosion behavior of CoCr porous coatings on orthopedic implants. *J Biomed Mater Res* 1998, 39: 292-299.

Puleo DA and Huh WW. Acute toxicity of metal ions in cultures of osteogenic cells derived from bone marrow stromal cells. *J Appl Biomater* 1995(6) 109-116.

Rae T. A study on the effects of particulate metals of orthopedic interest on murine macrophages *in vitro*. *J Bone Joint Surg*. 1975; 57-B (4); p444-50.

Ratner BD.(Ed) Biomaterials Science: An introduction to materials in medicine. Chapter 4. Academic Press. 1996.

Ryhanen J, Niemi E, Serlo W, Niemela E, Sandvik P, Pernu H, Salo T. Biocompatibility of nickel-titanium shape memory metal and its corrosion behavior in human cell cultures. *J Biomed Mater Res.* 1997, 15; 35(4): 451-7.

Rostlund T, Thomsen P, Bjursten LM, Ericson LE Difference in tissue response to nitrogen-ion-implanted titanium and c.p. titanium in the abdominal wall of the rat. *J Biomed Mater Res* 1990;24(7):847-60.

Riancho JA, Salas E, Zarrabeitia MT, Olmos JM, Amado JA, Fernandez-Luna JL, Gonzalez-Macias J. Expression and functional role of nitric oxide synthase in osteoblast-like cells. *J Bone Miner Res* 1995. 10(3): 439-446.

Savarino L, Granchi D, Ciapetti G, Stea S, Donati ME, Zinghi G, Fontanesi G, Rotini R, Montanaro L. Effects of metal ions on white blood cells of patients with failed total joint arthroplasties. *J Biomed Mater Res* 1999; 47(4): 543-550.

Sawase T, Wennerberg A, Baba K, Tsuboi Y, Sennerby L, Johansson CB, Albrektsson T. Application of oxygen ion implantation to titanium surfaces: effects on surface characteristics, corrosion resistance, and bone response. *Clin Implant Dent Relat Res.* 2001;3(4):221-9.

Santerre JP, Labow RS, Boynton EL. The role of the macrophage in periprosthetic bone loss. *Can J Surg* 2000; 43(3): 173-179.

Schedle A, Samorapoompichit P, Fureder W, Rausch-Fan XH, Franz A, Sperr WR, Sperr W, Slavicek R, Simak S, Klepetko W, Ellinger A, Ghannadan M, Baghestanian M, Valent P. Metal ion-induced toxic histamine release from human basophils and mast cells. *J Biomed Mater Res* 1998 Mar 15; 39(4):560-7.

Shabalovskaya SA. Surface, corrosion and biocompatibility aspects of Nitinol as an implant material. *Biomed Mater Eng*. 2002;12(1):69-109.

Shanbhag A, Macaulay W, Stefanovic-Racic M, Rubash HE. Nitric oxide release by macrophages in response to particulate wear debris. *J Biomed Mater Res*. 1998 Sep 5; 41(3): 497-503.

Sibum H. Titanium and titanium alloys. Ullman's Encyclopedia of Industrial Chemistry. New York. VCH publishers 1985. p95-121.

Signorello LB, Ye W, Fryzek JP, Lipworth L, Fraumeni JF Jr, Blot WJ, McLaughlin JK, Nyren O. Nationwide study of cancer risk among hip replacement patients in Sweden. *J Natl Cancer Inst* 2001 Sep; 93(18): 1405-10.

Spron P and Peters-Goldern M. Hydrogen peroxide inhibits alveolar macrophage 5-lipoxygenase m etabolism in association with depletion of ATP. *J Biol Chem* 1988. 263(29): 14776-83.

Strandman E, Landt H. Oxidation resistance of dental chromium-cobalt alloys. *Quintessence Dent Technol* 1982; 6(1):67-74.

Sunderman FW, Hopfer SM, Swift T, Rezuke W, Ziebka L, Highman P, Edwards B, Folcik M and Gossling HR. Cobalt, Chromium and Nickel concentrations in body fluid of patients with porous-coated knee or hip prostheses. *J Orthop Res* 1989, 7(3): 307-315.

Sundgren J, Bodo P, Lundstrom I, Berggren A, Hellem S. Auger electron spectroscopic studies of stainless-steel implants. *J Biomed Mater Res* 1985, 19(6): 663-71.

Sundgren JE. Auger electron spectroscopic studies of the interface between human tissue and implants of titanium and stainless steel. *J Colloid Interface Sci* 1986. 110: p9-20.

Suzuki R and Frangos J. Inhibition of inflammatory species by titanium surfaces. *Clinical Orthopedics and Related Research* 2000; 372: p280-289.

Tang L and Eaton JW. Inflammation responses to biomaterials. *Am J Clin Pathology* 1995; 103(4): 466-471.

Tengvall P, Elwing H, Sjoqvist L, Lundstrom I, Bjursten LM. Interaction between hydrogen peroxide and titanium: a possible role in the biocompatibility of titanium. *Biomaterials* 1989; 10 (March): 118-120.

Tengvall P, Lundstrom I, Sjoqvist L, Elwing H, Bjursten LM. Titanium-hydrogen peroxide interaction: model studies of the influence of the inflammatory response on titanium implants. *Biomaterials* 1989; 10 (April): 166-175.

Thompson G and Puleo D, Ti-6Al-4V ion solution inhibition of osteogenetic cell phenotype as a function of differentiation time course in vitro. *Biomaterials* 1996; 17(20): 1949-54.

Traisnel M, le Maguer D, Hildebrand HF, Iost A. Corrosion of surgical implants. *Clin Mater* 1990, 5, 309.

Trump BF, Valigorsky JM, Dees JH, Mergner WJ, Kim KM, Jones RT, Pendergrass RE, Garbus J, Cowley RA. Cellular change in human disease. A new method of pathological analysis. *Hum Pathol.* 1973 Mar; 4(1): 89-109.

van't Hof R and Ralston S. Cytokine-induced nitric oxide inhibits bone resorption by inducing apoptosis of osteoclast progenitors and suppressing osteoclast activity. *J Bone Miner Res* 1997. 12(11): 1797-1704.

Venugopalan R and Gaydon J. A review of corrosion behavior of surgical implant alloys. Princeton Applied Research technical review note 99-01.

Vezeau PJ, Koorbusch GF, Draughn RA, Keller JC. Effects of multiple sterilization on surface characteristics and in vitro biologic responses to titanium. *J Oral Maxillofac Surg* 1996 Jun; 54(6):738-46.

Wang JY, Wicklund BH, Gustilo RB, Tsukayama DT. Prosthetic metals impair murine immune response and cytokine release in vivo and in vitro, *J Orthop Res* 1997, 15(5): 688-699.

Wang JY, Wicklund BH, Gustilo RB, Tsukayama DT. Titanium, chromium and cobalt ions modulate the release of bone-associated cytokines by human monocytes/macrophages in vitro. *Biomaterials* 1996 Dec; 17(23): 2233-40.

Wataha JC, Lockwood PE, Marek M, Ghazi M. Ability of Ni-containing biomedical alloys to activate monocytes and endothelial cells in vitro. *J Biomed Mater Res* 1999 Jun 5; 45(3): 251-7.

Wataha JC, Lockwood PE, Khajotia SS, Turner R. Effect of pH on element release from dental casting alloys. *J Prosthet Dent* 1998, 80(6): 691-8.

Wataha JC, Hanks CT, Craig RG. The effect of cell monolayer density on the cytotoxicity of metal ions which are released from dental alloys. *Dent Mater* 1993; 9: 172-176.

Wataha JC, Nelson SK, Lockwood PE. Elemental release from dental casting alloys into biological media with and without protein. *Dent Mater* 2001 Sep; 17(5): 409-414.

Wataha JC, Ratanasathien S, Hanks CT, Sun Z. In vitro IL-1 beta and TNF-alpha release from THP-1 monocytes in response to metal ions. *Dent Mater* 1996 Nov; 12 (6): 322-7.

Wataha JC, Hanks CT and Sun Z. In vitro reaction of macrophages to metal ions from dental biomaterials. *Dent Mater* 1995 Jul; 11(4): 239-45.

Waters MD, Gardner DE, Aranyi C, Coffin DL. Metal toxicity for rabbit alveolar macrophages *in vitro*. *Environ Res* 1975. 9(1): 32-47.

Warner GL and Lawrence DA. The effect of metals on IL-2-released lymphocyte proliferation. *Int J Immunopharmac* 1988. 10(5):629-637.

Williams DF (Ed). Biocompatibility of Orthopedic Implants Vol 1, 1987; Chap 1 of biocompatibility, CRC Press, Inc.

William, DF. Biological properties of molybdenum. Systemic aspects of biocompatibility. Boca Raton, FL, CRC press, 1981.

Williams D and Clark G. The accelerated corrosion of pure metals by proteins. 7th Annu. Meeting Soc Biomaterials, 1981, p17.

Wink DA, Wink CB, Nims RW, and Ford PC. Oxidizing Intermediates Generated in the Fenton Reagent: Kinetic Arguments Against the Intermediacy of the Hydroxyl Radical. Molecular Mechanisms of Metal Toxicity and Carcinogenicity Environmental Health Perspectives 102, Supplement 3, September 1994.

Wooley PH, Petersen S, Song Z, Nasser S. Cellular immune responses to orthopedic implant materials following cemented total joint replacement, *J Orthop Res* 1997, 15 (6): 874-880.

Yamamoto A, Kohyama Y, Hanawa T., Mutagenicity evaluation of forty-one metal salts by the umu test. *J Biomed Mater Res* 2002 Jan; 59(1): 176-83.

Zardiackas L, Michell DW and Disegi JA. Characterization of Ti-15Mo beta Ti alloy for orthopedic implant applications. Medical Application of Titanium and Its Alloys: The Material and Biological Issues, ASTM STP 1272, S Brown and J Lemons, Eds, American Society fir Testing Materials 1996.

Zhu J, Xu N, Zhang C. Characteristics of copper corrosion in simulated uterine fluid in the presence of protein. *Adv Contracept* 1999;15(3):179-90.